LIGO Laboratory / LIGO Scientific Collaboration

LIGO-T0900649-v4 aLIGO February 2010

PSL Final Design

Hyunjoo Kim, Peter King, Christina Krämer, Patrick Kwee, Jan Pöld,
Richard Savage, Peter Weßels, Benno Willke

Distribution of this document:
LIGO Scientific Collaboration

This is an internal working note
of the LIGO Laboratory.

Albert-Einstein-Institut
Callinstraße 38
Hannover, D-30167
Federal Republic of Germany
Phone (05 11) 762 2229
FAX (05 11) 762 2784

California Institute of Technology
LIGO Project – MS 18-34
1200 E. California Blvd.
Pasadena, CA 91125
Phone (626) 395-2129
FAX (626) 304-9834
E-mail: info@ligo.caltech.edu

Laser Zentrum Hannover
Hollerithallee 8
Hannover, D-30419
Federal Republic of Germany
Phone (05 11) 27 88 0
FAX (05 11) 27 88 100
E-mail: info@lzh.de

Massachusetts Institute of Technology
LIGO Project – NW22-295
185 Albany St
Cambridge, MA 02139
Phone (617) 253-4824
FAX (617) 253-7014
E-mail: info@ligo.mit.edu

LIGO Hanford Observatory
P.O. Box 159
Richland, WA 99352
Phone (509) 372-8106
FAX (509) 372-8137

LIGO Livingston Observatory
P.O. Box 940
Livingston, LA 70754
Phone (225) 686-3100
FAX (225) 686-7189

http://www.ligo.caltech.edu/

Table of Contents

1 System Overview

1.1 Purpose

This document along with supporting analysis and detailed layout documents presents the final design for the Advanced LIGO (aLIGO) Pre-stabilized Laser (PSL) subsystem. The design information in this document supersedes that presented in the *PSL Preliminary Design* LIGO-T080195-v1 and is intended to present a detailed final design which conforms to the *Advanced LIGO PSL Design Requirements,* LIGO-T050036-v2. The intended audience for this document is the Advanced LIGO Detector Group. This overview section will give a high level description of the full PSL to lay the foundation for a better understanding of the following sections which will describe the different parts of the PSL in detail.

1.2 Introduction

The Pre-stabilized Laser (PSL) subsystem consists of the following elements:

- The Advanced LIGO Laser, including power supplies, the cooling system, internal diagnostics, its computer control system and the injection locking control electronics.
- A bow-tie shaped pre-modecleaner (PMC) to spatially and temporally filter the output of the Advanced LIGO Laser. The PMC is housed in a sealed vessel to reduce environmental disturbances and contamination of the mirror surfaces.
- The frequency stabilization control loop utilizing a rigid reference cavity, suspended in vacuum on a vibration isolation stack, as a frequency discriminator and an electro-optic modulator for fast frequency correction. Slower signals are fed back to the master laser piezo-electric transducer (PZT) and temperature control actuator.
- GW-band power stabilization of the light exiting the suspended modecleaner and entering the LIGO interferometer. This will include a high power photodetector placed downstream of the suspended modecleaner. This photodetector will be mounted inside the vacuum envelope on a seismic isolation table (HAM-ISI).
- A diagnostic breadboard to analyze the spatial beam profile, free-running frequency noise and power noise of the 35 W front-end laser and of the high-power oscillator.
- All computers, interface modules and software required to control the PSL and to provide the data interfaces to other detector subsystems and to the aLIGO data acquisition system.

It does not include:

- Mode matching lenses or steering mirrors that are part of the Input Optics (IO) detector subsystem.
- Electro-optic modulators for sideband frequencies utilized outside of the PSL subsystem.
- The interferometer input power level control (IO scope).

The PSL has interfaces to the

- IO, CDS, LSC and FMP subsystems.

1.3 Features / Capabilities

The main purpose of the PSL subsystem is to provide 165 W of stable 1064 nm laser radiation in a TEM_{00} spatial mode at a well defined optical interface to the IO subsystem. According to the most recent version of the DRD LIGO-T050036-v2 the required beam parameters at this interface can be found in Table 1.

Property	Value	Comment
Wavelength	1064 nm	Same as initial LIGO
Fundamental Mode Power	≥ 165 W	At the IO interface, in a circular TEM_{00} mode
Higher-order Mode Power	≤ 5 W	
Polarization	horizontal, > 100:1 ratio	At IO interface, polarization parallel to table surface, to ±1 deg
Beam size	550 µm	Beam waist at IO interface
Beam height	4 inches	At IO interface, from table surface
Alignment tolerance	± 2 deg	With respect to the vertical plane defined by the table surface

Table 1. Requirements for the PSL beam, as delivered to the IO subsystem.

The laser beam needs to be pre-stabilized in frequency and power and the PSL subsystem has to provide a wideband input for the IO frequency control actuator. The power stabilization of the beam downstream of the suspended modecleaner is in the scope of the PSL subsystem such that PSL photodiodes have to be placed into the vacuum envelope on the HAM 2 table. A diagnostic breadboard (DBB) is part of the PSL which allows a fast and automated characterization of the most important beam parameters.

To ensure a high reliability and availability the PSL needs to be operated in a extremely clean environment. Hence the PSL will be installed in a Laser Area Enclosure (LAE) which ensures a low particle count in the surroundings of the laser. To reduce environmental disturbances this room provides shielding against acoustic noise sources. A versatile air handling system will be installed which can provide large air exchange rates during installation and maintenance work and minimal flow during Science Mode. The LAE will be located near the HAM 1 chamber.

Most of the PSL electronics is placed in 19'' racks located outside of this room. Only servo electronics with high bandwidth requirements, computers for laser and PSL control and video monitors and cameras will be placed in the LAE. The computers and video monitors will be shutdown during Science Runs.

The acoustically noisy chillers for the laser system will be placed in the ante-room of the Laser Diode Room (LDR). The power supplies of the laser diodes will be installed in the

LDR. This arrangement will avoid electrical disturbances caused by the high current, switching power supplies to other sensitive electronics located in the Laser and Vacuum Equipment Area (LVEA). The laser diodes will be installed in close proximity to their power supplies. Metal jacketed optical fibers will deliver the pump light to the laser table where the light is used to pump the Nd:YAG and Nd:YVO_4 crystals. This reduces the length of cables carrying large currents, reduces the amount of cooling water needed in the LAE and will allow the exchange of laser diodes during a Science Run without entering the LVEA.

The LDR is required for the dual reasons of laser safety and cleanliness. A sketch of the distribution of the PSL components in the building can be found in Figure 1. The balloons indicate the internal and external interfaces of the PSL, which will be described later.

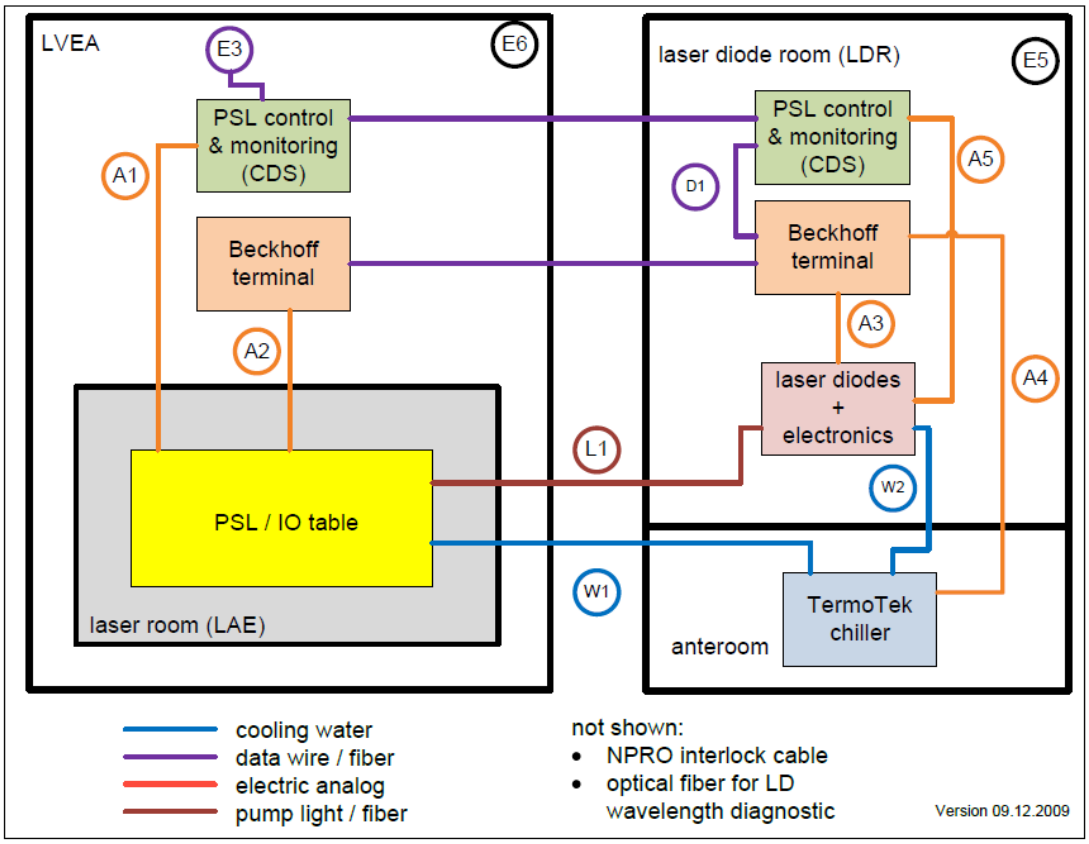

Figure 1. Arrangement of the different PSL components in the different locations. The laser bench is located in the Laser Area Enclosure, the control and DAQ computer are located outside of the Laser Area Enclosure in the LVEA and the laser diodes and noisy chillers will be placed into the laser diode room.

As with the iLIGO PSL and eLGO PSL, the aLIGO PSL shares an optical table with the IO subsystem. This optical table is the same one that was used for the iLIGO interferometers, a 16 ft. × 5 ft. × 24 in. thick Newport Research Series table. This table surface will be 40" above the LVEA floor such that a periscope is required to inject the beam into the vacuum system. The table support falls in the scope of the Facilities Modification and

Preparation (FMP) subsystem and the exact position of the PSL table within the LVEA coordinates system will be defined by IO.[1]

[1] At the time of writing this draft, the exact coordinates of the table have not been finalised.

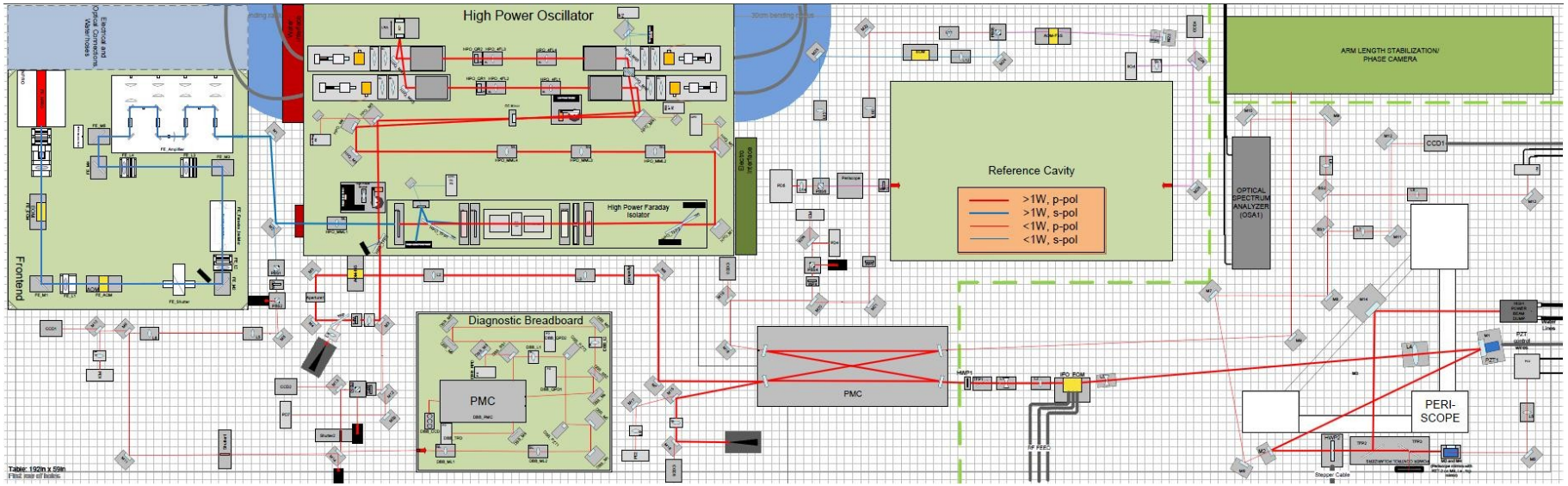

Figure 2. Schematic layout of the optics and electro-optical components on the optical table shared by the PSL and IO subsystem (IO components are shown for reference only. The relevant document for IO components is the IO final design document). The dashed green line approximately defines the border between the IO and PSL subsystem. A high resolution version of this figure is available as "PSL/IO table layout" (LIGO T0900610-v1) in the DCC.

The optical layout on this table and the arrangement of components is shown in Figure 2. A high resolution version of this diagram can be found under LIGO-T0900610. The laser consists of two units, the 35W front end laser and the high power laser (HPL). Both units come as separate boxes. An additional box contains the DBB components. The PMC is placed in an air tight aluminum container and the reference cavity is suspended within a vacuum container which is thermally isolated with Styrofoam pads. The eigenmode of the PMC defines the beam handed over to the IO subsystem and the pick-off beam for the IFO arm length stabilization unit and the phase camera unit.

A detailed description will be given in the following sections of this document.

1.4 Optical Layout and Control Strategy

A schematic sketch of the main PSL components and the relevant feed-back control loops is given in Figure 3. The PSL has four major sections:

- the high power aLIGO Laser,
- a frequency stabilization path including a rigid reference cavity and an acoustic optic modulator as an actuator for the second frequency stabilization loop,
- a PMC as a spatial filter and
- a diagnostic path that allows investigation of the laser behavior without interference with the PSL output beam.

The high power aLIGO Laser consists of a master oscillator, a 35W amplifier (identical to the eLIGO laser) and a high power injection-locked oscillator stage. An electro-optical modulator (EOM) is placed downstream of the master oscillator (NPRO) to provide a set of phase modulation sidebands that are required to produce error signals for control loops within the PSL (injection locking and the PMC length stabilization). The modulation frequency will be 35.5 MHz (the same as for iLIGO) which is a good compromise between being larger than the injection locking range and small compared to the free spectral range of the slave cavity. An additional EOM is needed in the frequency stabilization path to add the sidebands required for the Pound-Drever-Hall sensing at the reference cavity.

The frequency stabilization scheme is similar to the iLIGO scheme. Note that the beam directed toward the reference cavity for frequency stabilization is taken from one of the auxiliary ports of the PMC. This scheme has two advantages:

- The light incident on the reference cavity is closer to a pure TEM_{00} mode and hence the spurious noise effects of the higher order modes on the photodetector are reduced.
- The reference cavity control loop measures and suppresses any additional frequency noise added to the beam by the PMC and all optical components, such as mirror mounts, upstream of the pick off point.

A disadvantage of this scheme is that a loss of lock event of the PMC or the injection locking will kick the reference cavity out of lock and that the PMC pole needs to be compensated for in the frequency control loop filter. A diagnostic path will be part of the PSL that will allow for an online measurement of the beam parameters and the noise of either the 35 W front end or the high power stage.

The optical train of the PSL is kept as short as practicable with a minimum number of adjustable and fixed mirror mounts. All EOMs are mounted on four axis tilt aligners that enable alignment by moving the EOM rather than steering the beam into the EOM.

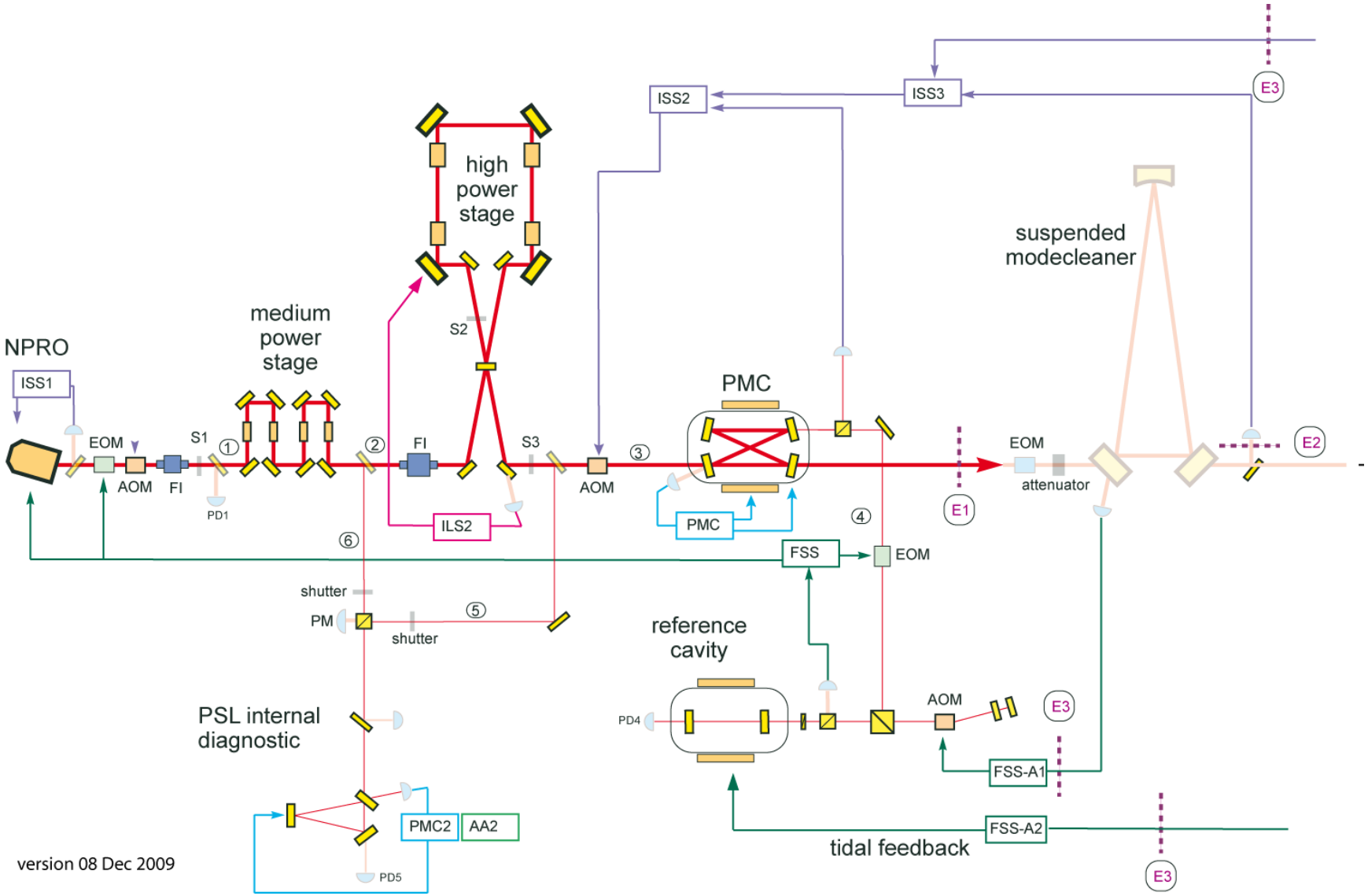

Figure 3. A schematic of the optical layout and control strategy of the PSL. AA: automatic alignment, ILS: injection locking servo, FSS: frequency stabilization servo, ISS: intensity stabilization servo.

1.5 Laser Safety

Laser safety is a very important consideration in the design of the aLIGO PSL. The highest risk exists during installation, commissioning and maintenance of the high power laser system. Careful planning of each work stage is required to avoid stray high power beams. Note that very high quality coatings will be required on all optical surfaces. The power transmitted when a 200 W beam is incident on a high reflectance (HR) coating with a transmittance of around 10^{-3} will be in the order of several hundred milliwatts.

Even though only trained and authorized personnel will be permitted to work on the laser, some stray beams are unavoidable during installation, commissioning and maintenance especially when work is performed on the high-power laser and the lid of its housing is open. Hence a room around the PSL table is required.

The official laser safety plan is not part of the PSL subsystem's scope, however the PSL safety plan is detailed in the aLIGO PSL Safety Plan LIGO-T0900614-v1.

1.6 Facilities Interfaces

The PSL will rely on the LIGO facility for the supply of mains electrical power, temperature and humidity control, HEPA filtered air, and space. In particular the ante-room of the LDR needs a powerful air-conditioning system to remove the heat transferred by the chillers from the cooling water into the air. This system was already installed prior to the eLIGO operation and will fulfill the requirements for the aLIGO PSL. In addition the PSL will rely on the LIGO facility to provide camera views of both the LAE and LDR. This will allow remote monitoring of either areas for reasons of safety and personnel location.

1.7 Remote Control

All PSL controls will be activated via the real-time CDS/RTLinux system. The controls internal to the aLIGO Laser (for example, the laser diode temperature control, laser diode current control, safety and internal diagnostics) will be a stand-alone system with a monitoring interface to the CDS system. The performance of the PSL will be monitored continuously and logged to allow comparison with previous performance levels. The CDS computer will also guide the various steps in the lock acquisition sequence and will generate alarms in case of a malfunction in the PSL.

1.8 Metric/Imperial Components

To avoid any confusion between metric and imperial units, components in all closed boxes provided by AEI/LZH will be metric, for example the 35 W front end, high power stage, diagnostic breadboard, PMC, laser diode boxes, control boxes, photodiodes provide by AEI. All components directly accessible on the laser table will use imperial units.

1.9 Components / designs to be reused from iLIGO or eLIGO

The aLIGO PSL will reuse the following components from iLIGO / eLIGO:

- the reference cavity including the vacuum container, ion pump and pressure gauges
- frequency shifter (EOM, AOM)
- tidal actuator (including electronics)
- 4 x 6HU crates
- 19” instrumentation racks
- optical table

The following components will be reused from eLIGO:

- 35W laser (after refurbishment)
- table top frequency stabilization servo

All hardware to be reused will be tested before or directly after installation in the aLIGO PSL subsystem. All design changes made for eLIGO will be incorporated.

2 The Advanced LIGO Laser

2.1 Overview

The final design for the aLIGO Laser is based on an injection-locked high power ring resonator (see Figure 4). This resonator contains four end pumped laser heads, where two of these heads are combined with a birefringence compensation scheme. In comparison to a MOPA scheme, stabilization of the optical resonator length is necessary. For this, the Pound-Drever-Hall injection locking scheme is applied. The stability requirements for the optical resonator length are given by the locking range of the oscillator which is a function of the ratio of resonator internal laser power and the power injected into the laser oscillator. Therefore, a double stage concept is realized. The first stage consists of a master oscillator power amplifier (MOPA) to increase the power of the master. The second stage, the high power laser (Slave), is injection locked to the first part.

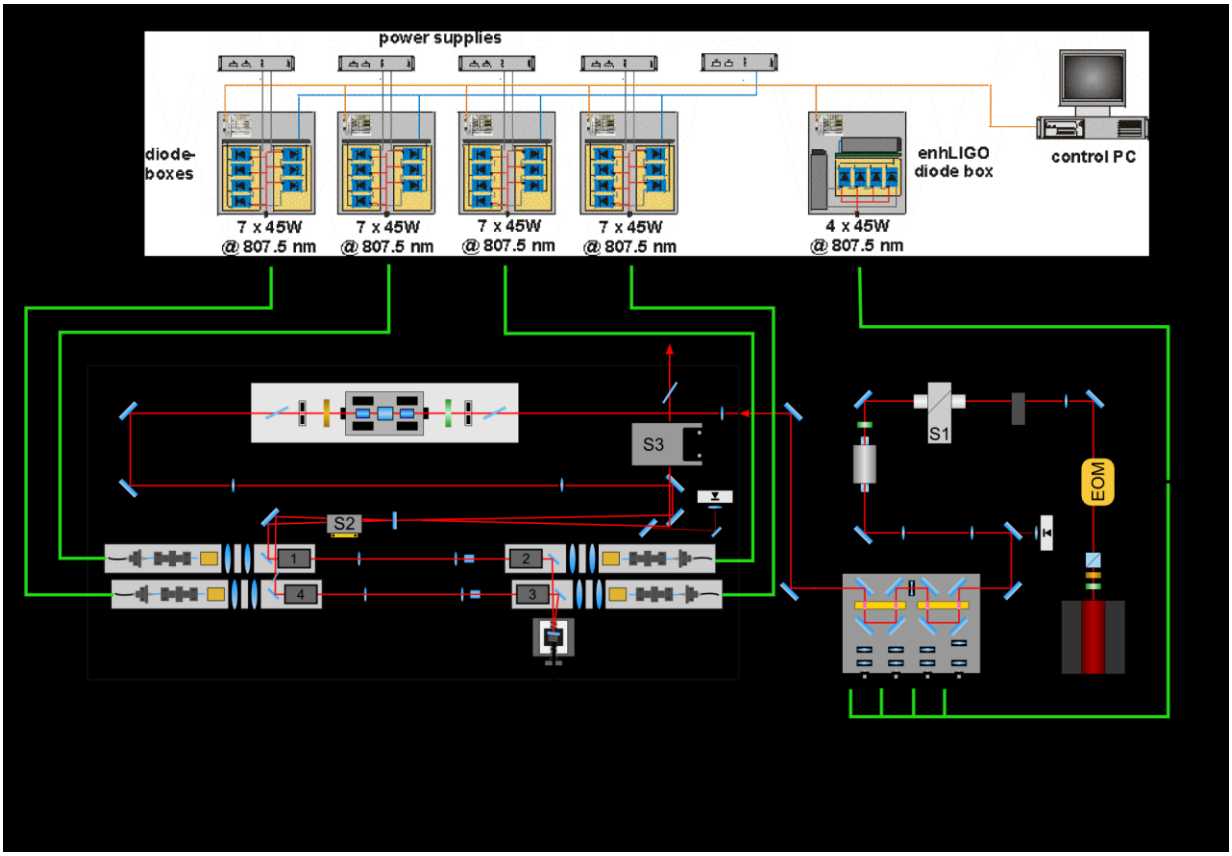

Figure 4. Schematic of aLIGO laser showing a single-frequency master laser, the 35 W laser followed by the high-power stage (Slave). EOM, electro-optic modulator. S1, S2, S3, shutters. FI, Faraday isolator. PD, photodiode. HPFI, high power Faraday isolator. MM1, MM2, mode matching lenses. OC, output coupling mirror. TFP, thin film polarizer. IL-PD injection locking photodiode. QR, 90° quartz rotator. PZT, resonator mirror mounted on piezo electric transducer. LRA, long range actuator.

A 2 W InnoLight Mephisto non-planar monolithic ring oscillator (NPRO) is amplified by a four head Nd:YVO_4 laser amplifier to a power level of 35 W. Typically more than 93 % of the 35 W laser beam is in the TEM_{00} mode. This stage is already used for the eLIGO PSL.

The light from the 35 W laser is then injected into the high power Nd:YAG oscillator to produce 200 W of output power. The length of the slave oscillator cavity is stabilized by employing the Pound-Drever-Hall stabilization scheme. This double-stage concept increases the locking range of the high power laser by a factor of 4 compared with directly locking it to the 2 W NPRO, which relaxes the resonator length stability requirements for the high power laser.

2.2 Target Specifications

The aLIGO PSL consists of a high power laser and the components used to pre-stabilize its free-running frequency and power. Based on the experience with a 200 W test bed operated at LZH and based on the experiences in the achievable loop gain for the stabilization schemes the target requirements for the free-running laser are listed in Table 2.

Parameter	Specification
1. type of laser	Nd:YAG, Nd:YVO_4
2. wavelength	1064 nm
3. output power	>200 W
4. power in higher order modes	< 20 W
5. polarization extinction ratio	100:1 in the vertical plane
6. relative power fluctuations	< 10^{-2} / √Hz between 0.1 Hz and 10 Hz < 10^{-5} / √Hz between 10 Hz and 10 kHz < 3.6 × 10^{-9} / √Hz for f > 9 MHz (3 dB above shot noise of 50mA photocurrent)
7. frequency fluctuations	< 1 × 10^{4} Hz / √Hz × [1 Hz / f] between 1 Hz and 10 kHz (same as NPRO free running)

Table 2. The aLIGO Laser target requirements.

2.3 Laser Design

The different components of the aLIGO Laser are described in the following sections. First, the front end is described, followed by a description of the high power oscillator stage.

2.3.1 35 W Front End

The light of the NPRO is phase modulated by an EOM, passes an AOM and a Faraday isolator and is then amplified in a single pass through 4 amplifier heads to 35 W. The gain material Nd:YVO_4 is chosen because of its high gain and natural birefringence which avoids depolarization effects. An end-pumping configuration is used in order to have good control of the overlap between the pump light and the laser mode which results in efficient amplification whilst preserving the excellent beam quality of the NPRO. A detailed description of the setup can be found in Frede et. al[2].

[2] M. Frede, B. Schulz, R. Wilhelm, F. Seifert, P. Kwee, B. Willke, D. Kracht, "Fundamental mode, single-frequency laser amplifier for gravitational wave detectors", Optics Express **15**, 459 — 465 (2007).

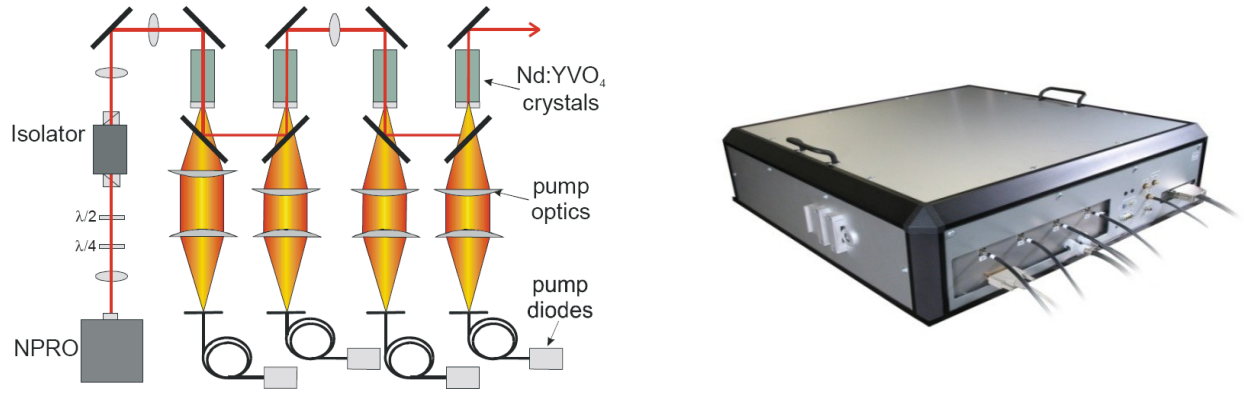

Figure 5. The 35W laser, left: Schematic layout of the setup, right: Actual realization.

The aLIGO front end is already used as the eLIGO Laser system. All of these lasers have already been built (1× Engineering Prototype at Caltech; 1× Reference System at the AEI; 3× Observatory, Hanford and Livingston and 2× spares). All these lasers are well characterized and proven for their use in the LIGO detectors. The eLIGO Laser and the aLIGO Laser are controlled by a Beckhoff real-time industrial control system which allows an easy implementation for the aLIGO front end.

2.3.2 High Power Stage

The high-power laser is based on a ring resonator design with four end-pumped laser heads, (see Section 2.3.2.1). Thermally induced mechanical stress in the Nd:YAG laser rods results in stress induced birefringence and causes depolarization and bifocussing. The stress induced birefringence can be compensated for by two identically pumped rods and a 90° quartz rotator. A relay optic, consisting of two identical lenses, images the principal planes of the rods onto each other whilst keeping the laser field unmodified. Therefore nearly perfect birefringence compensation can be achieved[3]. In the high power stage, two birefringence compensated pairs of laser heads are assembled to form a ring resonator cavity, as illustrated in Figure 6.

[3] M. Frede, R. Wilhelm, M. Brendel, C. Fallnich, F. Seifert, B. Willke, and K. Danzmann, "High power fundamental mode Nd:YAG laser with efficient birefringence compensation", Optics Express **12**, 3581 — 3589 (2004).

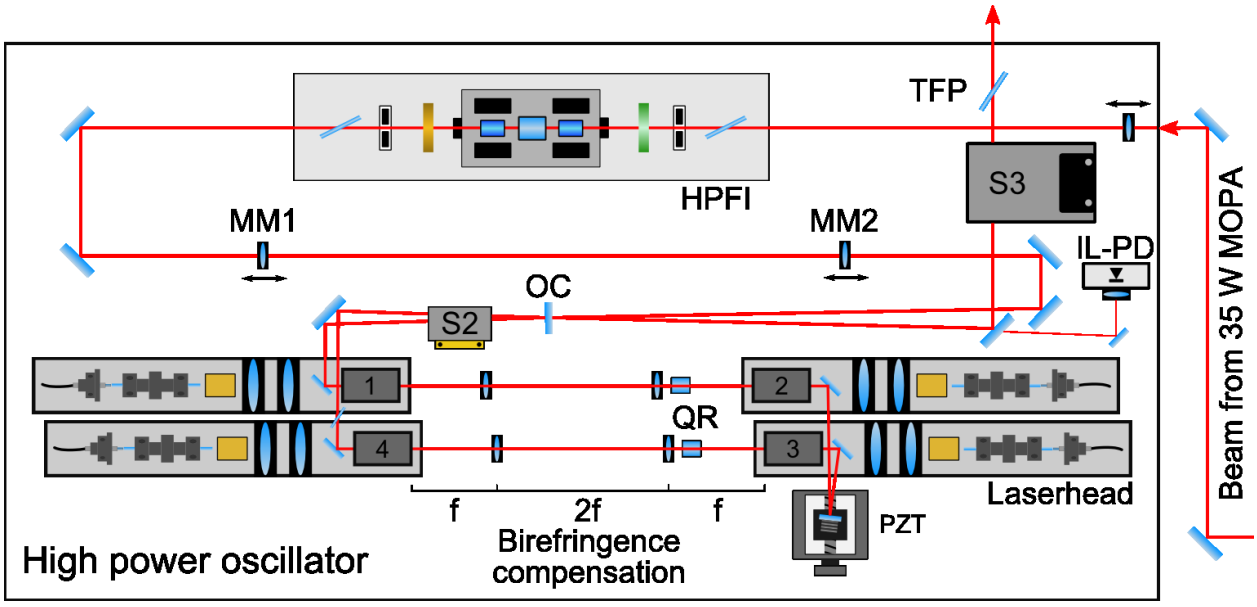

Figure 6. Schematic layout of the high power ring laser oscillator including the high power Faraday isolator and the two shutters S2 and S3. OC, output coupling mirror. MM1, MM2 mode matching lenses. TFP, thin film polarizer. HPFI, high power Faraday isolator. IL-PD, injection locking photodiode.

With this setup a laser output power of about 175 W of the non-injection locked laser in a linearly polarized fundamental mode operation was demonstrated with the Engineering Prototype.

2.3.2.1 End Pumped Laser Head

Each of the four laser crystals is pumped by 7 fiber-coupled laser diodes, each with a nominal power of 45 W and a wavelength around 807 nm. The laser diodes are individually temperature stabilized which ensures a narrow emission spectrum in the range of 2–3 nm FWHM of the fiber bundle. Operating the laser diodes at a derated output power of about 80 % of their nominal power improves diode lifetime and reliability. The specified lifetime at full power is about 20,000 hours (~27 months) during which less than a 20 % increase in driving current is needed to keep the output power constant.

The pump light is delivered by a fiber bundle of 7 fibers with 400 µm core diameter, NA 0.22 each. One end of the fiber bundle is attached with a bare fiber SMA905 connector to the laser diodes. On the other end the bare fibers are glued in an aluminum holder and mounted onto the laser head. If the light from the fiber bundle was directly imaged into the laser rod, hot spots due to the inhomogeneous pump light distribution would occur. For this reason, a fused silica rod homogenizes the transverse pump light distribution of the seven incoming fibers due to the spatial mixing of the light rays emerging from different fibers. By this homogenization, the formation of hot spots

due to the direct imaging of the fiber bundle is prevented. In addition, this ensures a nearly unchanged pump light profile in case of a pump diode failure or degradation.

A two lens optic images the end surface of the homogenizer into the laser crystal (see Figure 7).

The laser crystal consists of a 3 mm diameter multi-segmented Nd:YAG rod with two 7 mm long undoped segments at both ends and a 40 mm long low-doped center segment. The undoped end caps reduce the thermally induced mechanical stress on the end surfaces of the rod and eliminate any mechanical deformation of the ends. Furthermore, the entire doped central region of the rod can be effectively cooled, which is essential for the end-pumped geometry in connection with direct water cooling.

The coupled pump light is mixed and guided by total internal reflection at the rod surface during propagation. A coating for a pump light double pass is applied to the backplane of the crystal to reduce the longitudinal thermal gradient and the overall mechanical length.

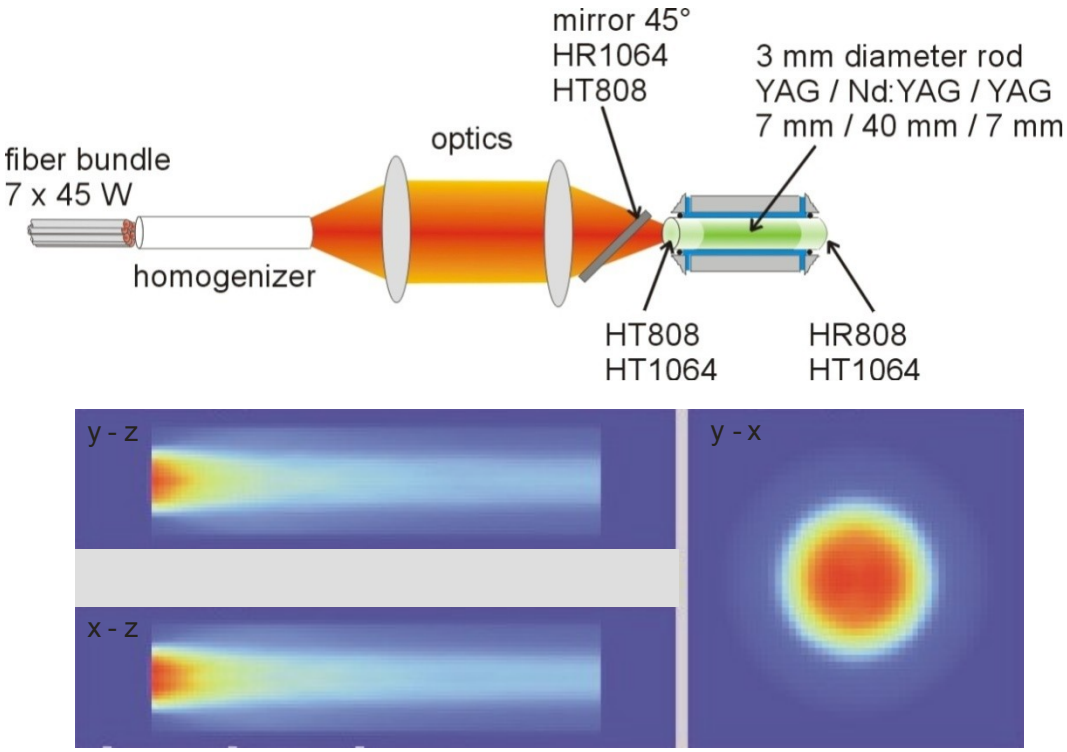

Figure 7. Schematic layout and pump light distribution in the end-pumped laser head.

2.3.2.2 Resonator Design For Fundamental Mode Operation

Scaling the laser power by increasing the pump power introduces thermally induced aberrations in the crystals due to the temperature dependence of the crystal material properties such as thermal conductivity and thermally induced refractive index changes. By keeping the average temperature in the rod below 60°C, thermally induced

aberrations are drastically reduced. The second source of aberrations is the pump light distribution, which is concentrated near the rod-axis (see Figure 7). This results in spherical aberrations that are responsible for a thermal lens that depends on the incident laser beam radius and therefore on the mode size. The laser resonator was designed to use these spherical aberrations as a control mechanism for the fundamental mode operation of the laser system. An asymmetric resonator was designed to split the resonator stability range in two parts with respect to the applied pump power. Furthermore, due to the aspherical thermal lens inside the crystals, the higher order modes experience a lower effective thermal lens than the fundamental mode due to their larger mode field diameter. By choosing the right cavity parameters, a working point where only the TEM_{00} mode is stable can be found at the beginning of the second stability range (see Figure 8). In the actual resonator design this working point can be found at a pump power of approximately 250 W per laser head. The position with respect to pump power of the second stability range can be changed by varying the "short" length (Figure 6, right side, PZT mirror) whereas the mode size inside the cavity can be altered by changing the output coupler arm length of the resonator (Figure 6, left side / top of resonator). The TEM_{00} laser mode size is chosen to have a good overlap with the pump light and uses the laser crystals as an additional aperture to suppress higher order modes.

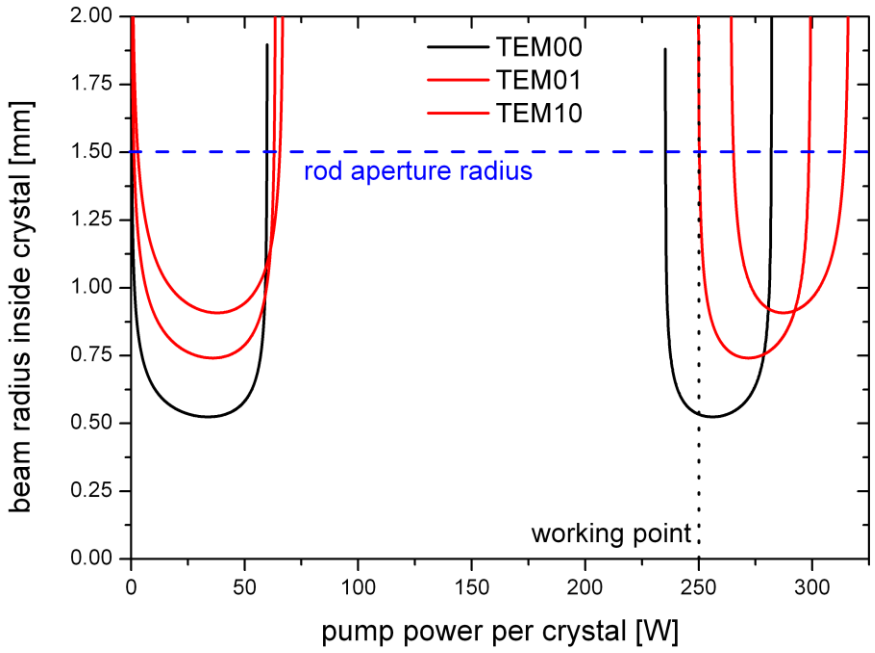

Figure 8. By use of an asymmetric resonator design only the TEM_{00} mode oscillates at a certain pump power range. At higher pump powers, higher order modes start to oscillate inside the cavity. At lower pump powers, the resonator is not stable.

2.3.3 Output Properties

A complete characterization of the Engineering Prototype operated at the AEI can be found in Engineering Prototype Performance document (low and high power mode) (LIGO T0900617-v1).

2.3.4 The High Power Oscillator Box

In the following, a detailed description of the components and subsystems inside the high power oscillator box will be given.

2.3.5 Systems Dimension

A system overview on the PSL Table and the dimensions can be seen in Section 1.3 and Figure 2. For a detailed view of the components inside the high power laser box see Figure 9.

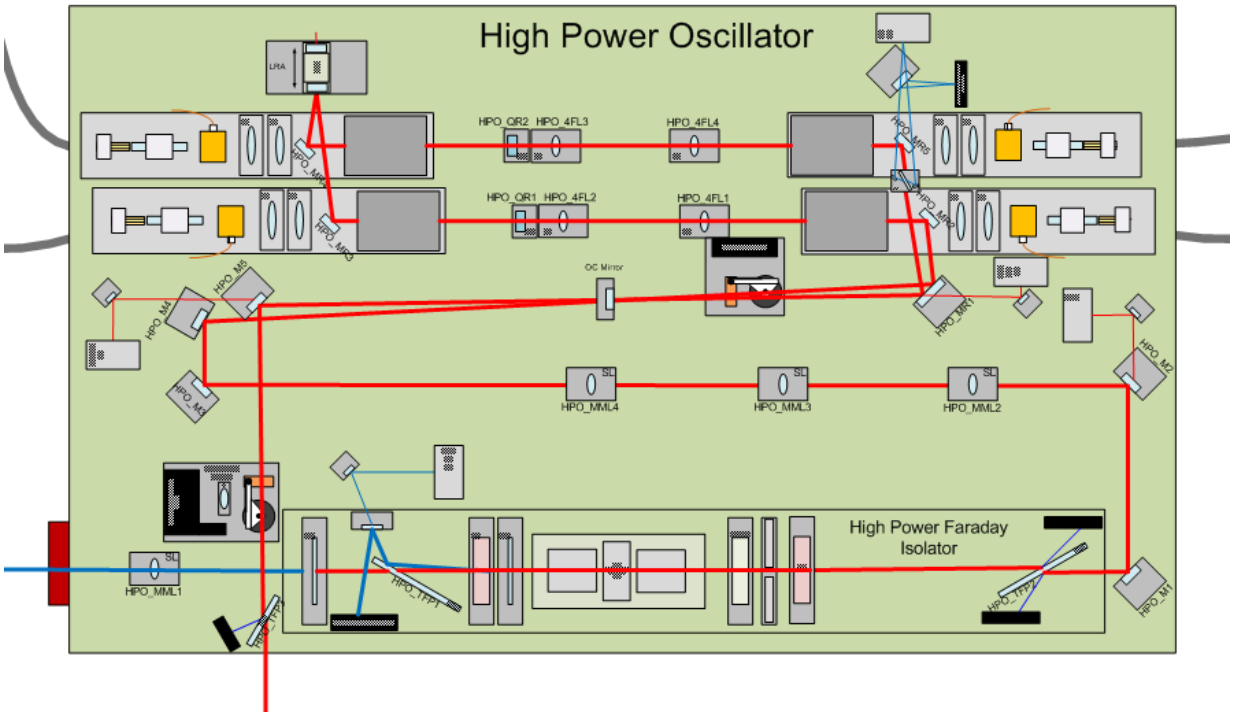

Figure 9. Detailed view of the setup inside the high power laser box.

The beam enters the box in the lower left corner (blue beam), is then collimated with a single lens and passes the high power Faraday isolator (see Section 2.3.7). It is then mode matched with 2 or 3 lenses and coupled into the high power oscillator cavity through the output coupling mirror in the middle of the box. Inside the resonator, the beam passes through the four laser heads, the 4-f imaging optics and the quartz rotators, and the long range actuator with the PZT mirror (see Section 2.3.12). In addition, inside the resonator, the low power shutter can be found (see Section 2.3.8). Before exiting the laser box, the beam passes through the high power shutter (see 2.3.9) and the power in the wrong polarization is rejected by a thin film polarizer.

In addition, some unwanted power in a kind of “corona” is filtered out by an aperture (not shown in the figure).

In Figure 10, a photograph of the actual realization (Engineering Prototype) of the high power laser is shown.

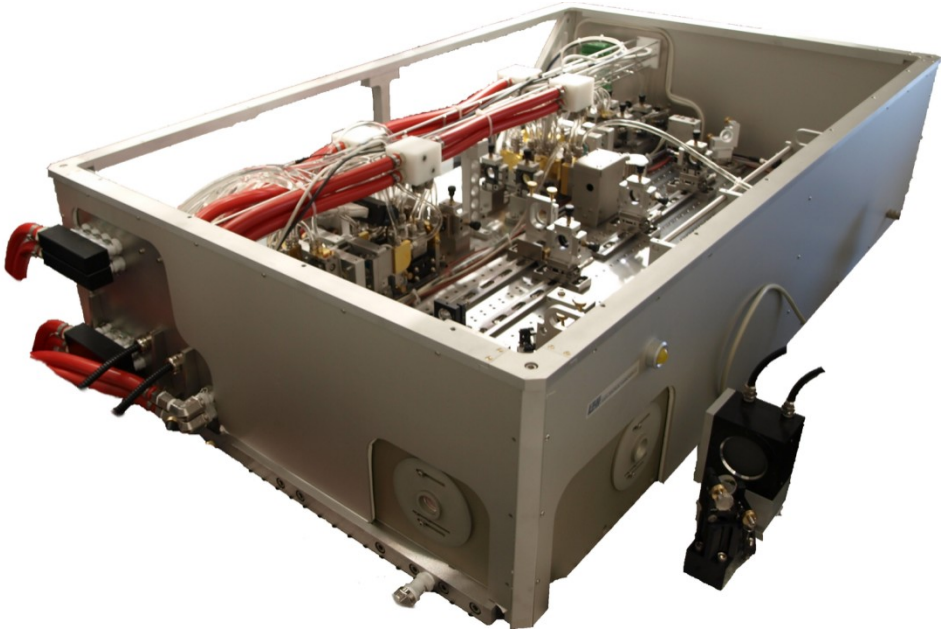

Figure 10. Hardware implementation of the High Power Laser (Engineering Prototype).

2.3.6 Choice of Materials

The materials for the various components have been selected according to different criteria. The oscillator base plate, the laser heads, and the Faraday isolator base plate are made out of stainless steel with a thermal expansion coefficient of 10.6 ppm/K which matches that of the optical table in order to minimize any thermal distortions of the laser system. In addition, all water exposed stainless steel components do not contain any molybdenum as experience with the Laboratory Prototype showed some molybdenum deposition on the laser crystals which are in direct contact with the water of the same circuit.

All components which come into contact with the cooling water have been chosen in order to avoid any corrosion. For example most of the heat sinks are made of gold plated copper, whilst the fiber bundle and homogenizer holders are made of hard anodized aluminum.

2.3.7 Faraday Isolator

The input Faraday isolator inside the high power oscillator box protects the 35 W MOPA from backwards propagating light from the unlocked oscillator. Because of the

approximately 120 W transmitted through the TGG[4] crystals inside the Faraday rotator, a thermal lens and depolarization evolve. These two effects lead to a changed propagation of the 35 W beam during lock acquisition and cause an unstable lock behavior. To compensate for this, two different methods are used inside the High Power Faraday Isolator (HPFI).

To compensate for depolarization effects, a 67° quartz rotator is placed in between the two 22.5° TGG crystals inside the Faraday rotator. To achieve a total polarization rotation of 180° in the direction of the 35 W beam and 90° backwards, a $\lambda/2$-plate is installed in front of the rotator. Secondly, a DKDP-plate is mounted after the Faraday rotator. Slightly absorbing at a wavelength of 1064 nm, DKDP produces a thermal lens with negative focal length. If the longitudinal dimension is matched to the absorption of the TGG and the quartz inside the rotator, the thermal effects inside the Faraday rotator can be compensated. To reach high isolation levels of the complete Faraday isolator, calcite wedges, which offer a polarization ratio of more than 1:10000, are used. The disadvantage of these polarizers is that the two output polarizations are only separated by a small angle. The beams can be just separated after a propagation distance of approximately 50 cm. To shorten the distance and to give the opportunity of analyzing and not only blocking the beam, Brewster angle thin film polarizers (TFP) are placed in front of the calcite wedges. With this combination of polarizing optics one can keep the good polarization ratio of the calcite and separate the beams with the TFP.

The Faraday rotator (consisting of the TGG crystals and the quartz rotator) and the matched DKDP crystals are commercially available from Molecular Technology GmbH. This company is the distributor for the Faraday rotators developed by Professor Efim Khazanov's group at the Institute of Applied Physics of the Russian Academy of Sciences.

2.3.8 Low Power Shutter / Low Power Mode

Two shutters are included inside the high power oscillator box. The low power shutter is located inside the high power laser resonator. If activated, this shutter blocks the beam path inside the oscillator. It is meant to be used if less than the maximum output power of the laser is needed, i.e. if the laser is to be operated in the low power / reduced power mode. In this mode, the high power oscillator is not operating. Thus, the output power of the system is reduced to the beam of the Front End that is reflected on the output coupling mirror (≥ 50 %). In order to save the pump diode life time, it is recommended that the high power laser is switched off if the system is to be used in the Low Power Mode for a long time.

2.3.9 High Power Shutter

This shutter can be activated, if no laser radiation is desired in the beam path following the oscillator box. For interruption of laser radiation for a short while this shutter can and should be used without powering down the laser diodes, since the laser will just be blocked, but not switched off. Thus, the complete system will stay in thermal equilibrium. If the laser power is not needed for a longer period (several days) it is

[4] Terbium gallium garnet.

recommended to shutdown the high power laser in order to save the pump diode life time. The activated shutter blocks the beam path to the outcoupling window of the laser box and deflects the beam to an internal power meter. The power which is measured here can be read out. Usually, it will be 3 to 4 W higher compared to the power which is emitted from the box, since an additional polarizer is mounted behind the shutter. The high power shutter will be closed automatically, if one of the interlocks trips. In this case the pump diodes will also be switched off and will need to be rebooted after elimination of the cause of the failure.

2.3.10 Laser Head Configuration

In Figure 11, a schematic of a single laser head is shown.

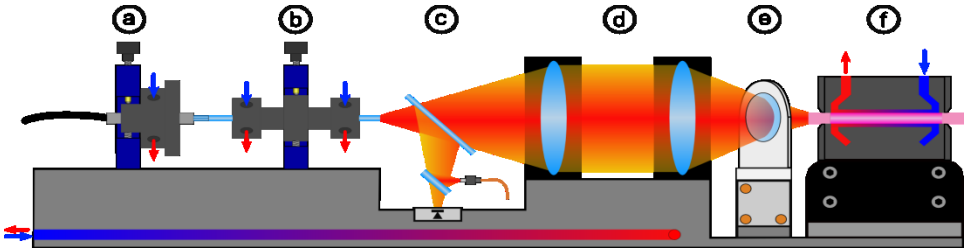

Figure 11. Schematic of the laser head.

The laser head consists of the following components:

a) Pump light fiber bundle holder. The seven pump fibers are glued into an aluminum holder which is screwed into a water cooled aluminum chamber. This is mounted in an x-y lens mount.

b) The homogenizer rod is mounted into an aluminum holder that is water cooled at both ends. The homogenizer does not come into contact with the water. The cooling chamber is mounted in an x-y lens mount.

c) A small part of the pump light is split off for diagnostic purposes (see Section 2.3.11).

d) The pump light is imaged with two lenses,

e) it passes through a dichroic mirror and

f) then focused into the laser crystal which is mounted inside a stainless steel cooling chamber. The laser crystal is directly water cooled. In order to enable a fine adjustment of the laser crystal with respect to the pump and laser beam, a 4 axis translation and tilt stage is used for mounting of each laser crystal.

All components that belong to a single laser head are separately mounted on a rigid water cooled stainless steel spacer allowing for easy resonator optimization and alignment without misaligning the pump setup (see Figure 12 for a single complete laser head assembly.)

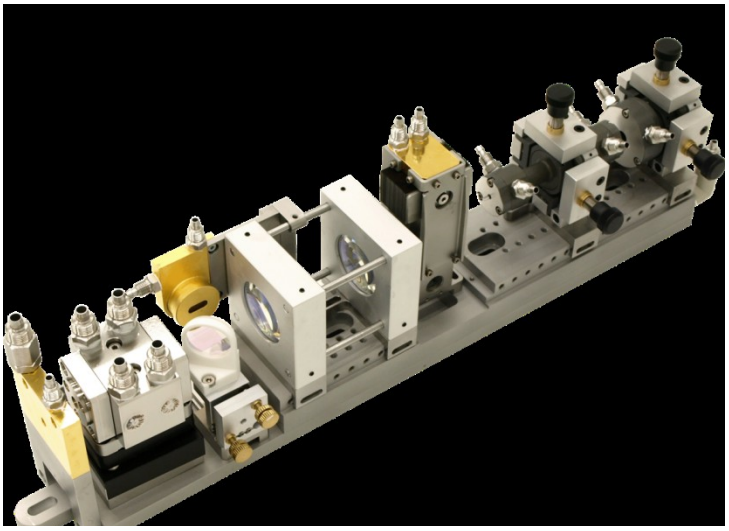

Figure 12. Actual realization of the laser head.

Behind the laser crystals a water cooled copper aperture is mounted to the laser head base plate in order to block the spontaneous emission but let the main laser beam pass through.

2.3.11 Pump light diagnostics

Having passed the homogenizer rod, a small fraction of the pump light is picked off by a 45° AR coated window, see Figure 11 (c). This fraction is then split into two parts. The main fraction is reflected and focused onto a 62.5 µm gradient index fiber. The smaller fraction is focused onto a monitoring photodiode.

IBS coatings are used to minimize the influence of humidity variations on the photodiode power read out.

The output from each of the four fiber bundles from the four laser heads is then fed into a 4×1 fiber optic switch. With this fiber optic switch the light from one of the four inputs is redirected to an output fiber which is coupled to an optical spectrum analyzer. This allows both the monitoring of the total pump power per laser head and a measurement of the pump light optical spectrum for each of the four individual laser heads.

2.3.12 Long range actuator

The PZT actuated mirror is mounted on a DC motorized stage (long range actuator, LRA) which is used to compensate for long term resonator length drifts due to temperature or air pressure. The voltage applied to the PZT is monitored and kept within a certain range by driving the stage in small and slow steps (about a µm per second when activated). Due to this slow speed, the PZT mirror is kept within its dynamic range while the system remains injection locked.

As a test, the room temperature at the AEI was increased by about 2.5°C by shutting off the air conditioning (see Figure 13). During this test, the LRA was automatically activated 8 times and the laser system remained in lock during the complete test.

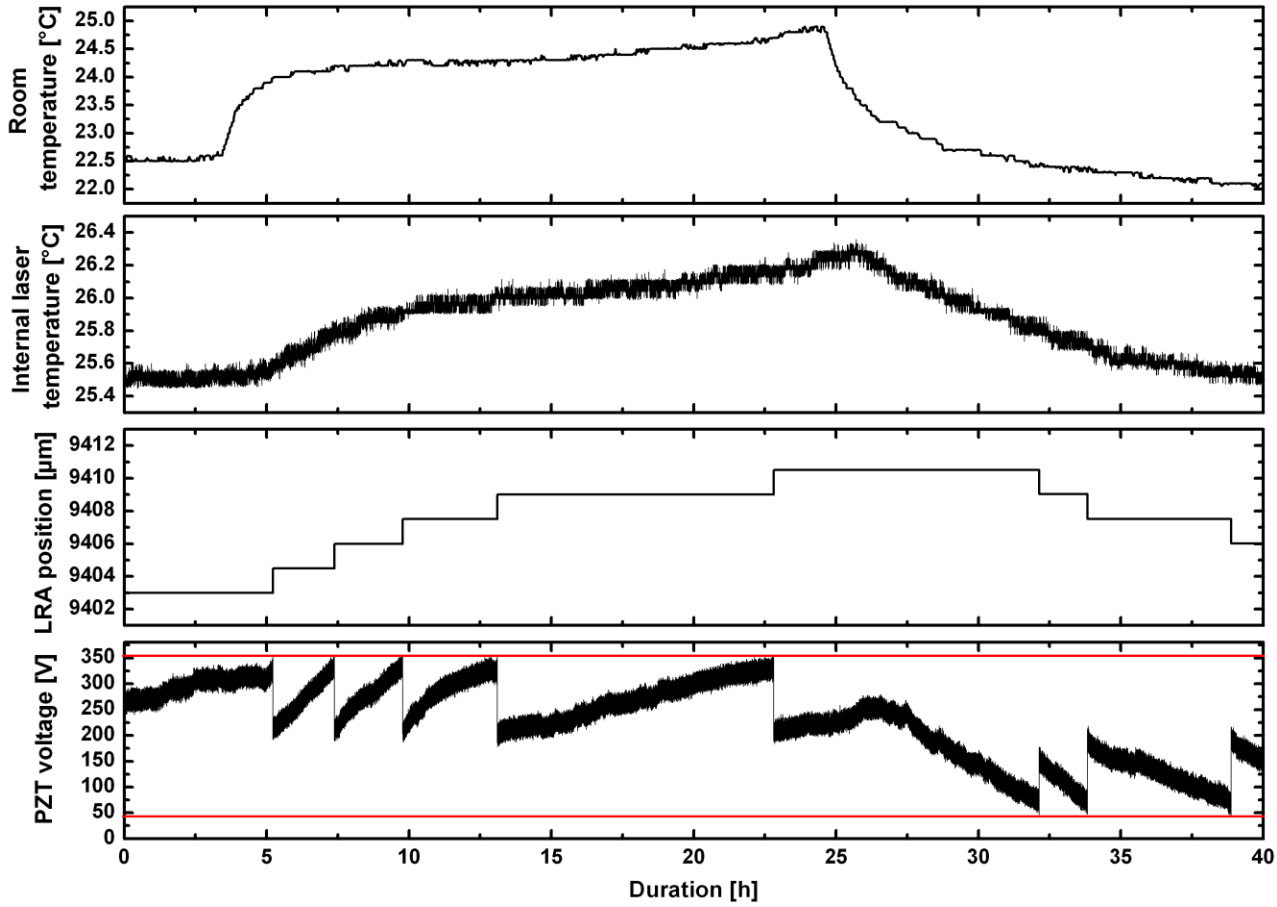

Figure 13. Test of the LRA. First graph: Room temperature measured with a sensor outside the laser box. Second graph: Temperature measured inside the laser box. Third graph: Position of the LRA. Fourth graph: Voltage applied to the PZT.

2.3.13 Water cooling inside the laser box

Almost all components that are exposed to laser radiation and thus could heat up during operation are water cooled to keep the system in thermal equilibrium and to minimize thermal expansion during the system start phase. In particular, the following components are directly water cooled:

- In the laser head (see Figure 11):
  - the holder for the hard-coated aluminum fiber bundle holder,
  - the holder for the hard-coated aluminum homogenizer holder,

- the beam dump in the pump light diagnostics,
- the pump light beam dump,
- the laser crystal cooling chamber,
- the ASE beam dump.

- The high and low power shutters
- The beam dumps for
  - The light in the wrong polarization reflected off the resonator internal Brewster plate and the output thin film polarizer,
  - The output mode aperture

Tests with the Engineering Prototype showed that water cooling of the oscillator box base plate is not necessary. During the temperature test shown in Figure 13, the base plate was not water cooled. No impact on the laser performance was observed.

2.3.14 Diagnostics / Sensors

The following sensors are implemented and monitored via Beckhoff and EPICS for diagnostic purposes inside the laser oscillator box:

- Temperature sensors:
  - 5× on the oscillator base plate
  - 4× on the laser heads (one on each)
  - 1× to measure to the air temperature inside the laser box
- 1 sensor for the relative air humidity inside the laser box. This sensor shall be used in combination with a room / environmental humidity sensor to detect small water leaks inside the laser box by comparing the two measurements.
- Photodiodes:
  - 4× in the pump light diagnostics
  - 1 injection locking photodiode
  - 1 at the resonator internal Brewster plate to measure the amount of depolarized power
  - 1 to measure the resonator internal power (behind the bending mirror in front of the output coupling mirror)
  - 1 to measure the input power from the front end (behind a bending mirror before the input into the high power oscillator)
  - 1 to measure to the backwards travelling power (installed in the backwards path in the high power Faraday isolator)
- 1 cooling water pressure sensor each in the water inlet and the water outlet in the water distribution for the oscillator and MOPA at the laser table

- Cooling water flow sensors:
  - 4× in the individual circuits to the 4 laser heads
  - 1× for the water flow in the Front End
  - 1× for the water in the beam dumps in the high power laser box

2.4 Opto-electronic Control

2.4.1 Computer control

The laser system is controlled via a software programmable logic controller (PLC, see Section 7.3 for more information). The laser parameters are monitored and controlled with decentralized I/O terminals utilizing an Ethernet bus technology. This makes it easy to upgrade and implement additional I/Os at various places into the system.

A graphical computer interface is provided via virtual network computing (VNC) that gives access to the main operating parameters for monitoring, controlling and diagnosis of the laser (see Figure 14 for the main control screen).

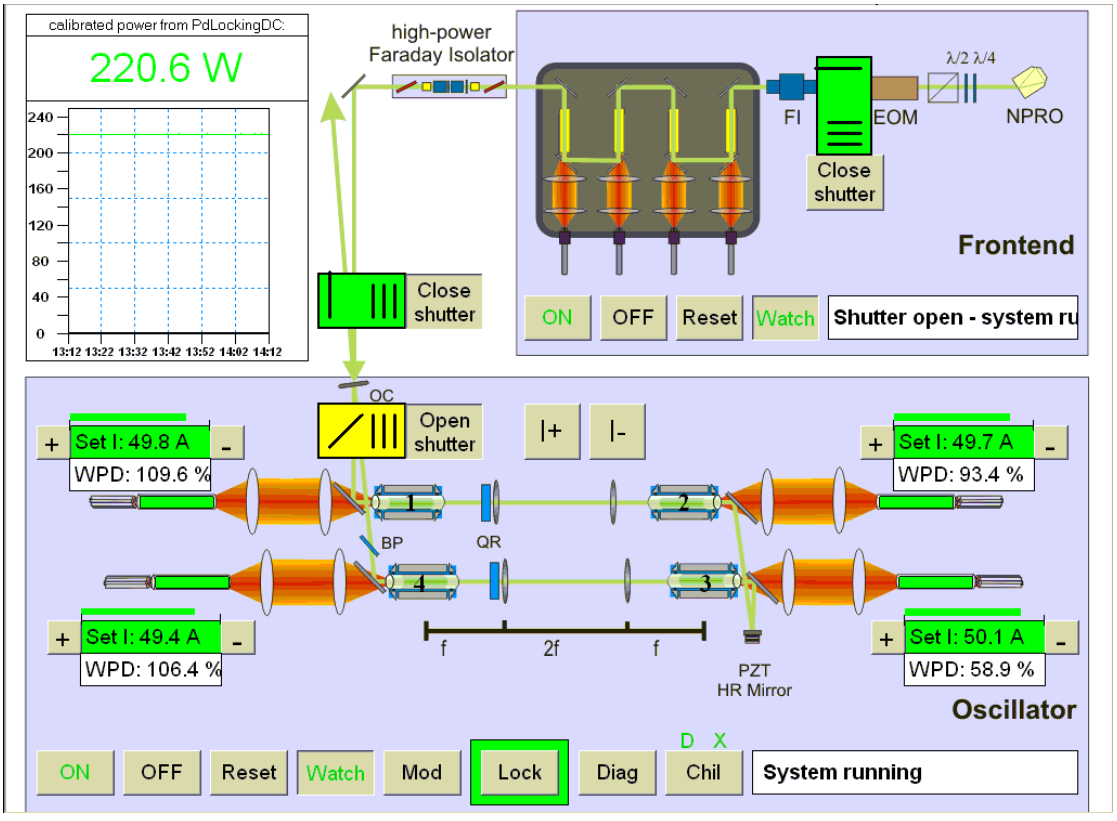

Figure 14. The graphical user interface accessible via VNC login to the laser computer.

2.4.2 Configuration of Laser Diodes and Power Supplies

Fiber delivery of the pump laser diode output allows the laser diodes and their power supplies to be remotely located from the laser (see Figure 1). The multimode optical fiber has losses of 4 dB/km at 808 nm, so locating the laser diodes 100 meters from the laser will only reduce the power delivered by 5%. Each laser diode nominally delivers 45 W of power and 28 diodes are needed for the high power oscillator and an additional 4 diodes are required for the 35 W laser. Each laser diode's temperature is controlled by a computer based proportional-integral-differential (PID) controller, which results in a temperature stability better than ±15 mK. With this temperature stability, additional noise resulting from variations of the total absorbed pump power due to pump wavelength changes can be neglected.

The diodes are operated in a derated condition to increase the diode lifetime. In general the operating point is 80% of the nominal diode working point. The diodes are powered in groups of 7 that are in series, thus 4 power supplies are required for pumping the high power stage. Two additional power supplies are needed for the Peltier elements used for the laser diode temperature stabilization. This number of commercial power supplies fits in a standard 19 in. rack that is 6 ft. tall. Due to the additional control electronics for the PSL system the electronics will be split between two racks, see Section 7.2 for an overview.

2.5 Water Cooling

The laser/amplifier heads in both the 35W front end and the high power stage (slave) require chilled water cooling. The master oscillator (NPRO) is not water cooled.

The PSL uses two water chillers by Termotek, one for the laser diode room (P605, 5 kW cooling capacity) and one for the laser room (P325, 1.7 kW cooling capacity). For the eLIGO phase, a loop made with ¾" schedule 80 LXT PVC pipe which is specially designed for ultra pure water systems and valves made of LXT PVC has been installed and can be reused. The chillers are air cooled and they exhaust all of their heat load into the ante room of the LDR, where it is removed by the local HVAC system.

Both chillers are built to be compatible with de-ionized water and are equipped with a de-ionizer cartridge that is designed to keep the conductivity of the water at about 4–7 µS/cm. The supply water temperature, pressure, and conductivity are continuously monitored and recorded by Beckhoff and EPICS. Water flows at both the laser chiller and the diode box chiller are also monitored and recorded.

The water chillers for the aLIGO Laser are located in the ante-room of the LDR (refer to Section 7.2). The chillers are controlled by the logging in to the control PC via VNC.

The chillers have a 2 liter internal water tank and will automatically shut down if the water level is too low. Thus, in case of a large water leak e.g. inside the laser box, the chiller will shut down at the latest after the loss of 2 liters of water even though there is much more water inside the water pipes available (this was tested successfully).

3 Frequency Stabilization System

3.1 Overview

The principal performance requirements of the aLIGO PSL frequency stabilization system fall into the following five categories:

- Long term (>100 sec) frequency stability
- Control band (0.1 – 10 Hz) frequency fluctuation levels
- GW band (10 Hz – 10 kHz) frequency noise levels
- Bandwidth and range of the *Wideband frequency input.*
- Range and response time of the *Tidal frequency input*

The first two requirement categories are new, while the last three are similar to, though generally less stringent than, the iLIGO requirements.

Although the aLIGO laser source is different than the iLIGO laser, the NPRO (non-planar ring oscillator) master oscillator is similar to that utilized by the iLIGO laser, so we expect similar free-running frequency noise performance. The aLIGO laser uses an NPRO manufactured by InnoLight in Hanover, while the iLIGO laser used an NPRO from Lightwave Electronics in Mountain View, CA. Experience with the 35-W Front End laser and the high-power injection-locked oscillator shows that the overall frequency noise is only about 5 dB above that of the NPRO (see Figure 16).

The frequency stabilization scheme for the aLIGO PSL is similar to that employed for the iLIGO PSL except that the sample of the laser output directed to the reference cavity is picked off downstream of the pre-modecleaner (PMC). For the iLIGO PSL it was picked off upstream.

The global interferometer frequency stabilization scheme employs nested loops utilizing the increasing frequency sensitivity of three Fabry-Perot cavities; the PSL reference cavity, the IO mode-cleaner, and the interferometer's long arm cavities using the LSC common-mode signal. The PSL frequency stabilization sensor utilizes a linear, fixed-spacer reference cavity that is suspended on a vibration isolation system inside a vacuum chamber. The three frequency actuators are i) control of the master oscillator (NPRO) temperature, commonly referred to as the SLOW actuator, ii) a PZT bonded to the oscillator crystal that changes the frequency via strain-induced optical path length changes, commonly referred to as the FAST actuator, and iii) high-speed control of the optical phase via an EOM located between the NPRO and the 35-W amplifier stage.

A *wideband frequency input* actuator is provided to the IO detector subsystem for further stabilization of frequency fluctuations. This input shifts the frequency of the sampled beam directed to the reference cavity via an AOM driven by a voltage-controlled oscillator (VCO). A *tidal frequency input* actuator is provided for very low-frequency correction via changes in the temperature of the reference cavity. Both of these actuators are similar in design to those utilized in the iLIGO PSL, and will of course utilize any improvements implemented during operation of the eLIGO PSL.

3.2 Long term frequency stability

The PSL frequency is required to be stable to within 1 MHz (or no less stable than the iLIGO PSL, whichever is more stringent) over time scales longer than 100 s. The frequency stability of the free-running laser met this requirement. D. Sigg and R. Savage working in a poorly controlled thermal environment at MIT, recently locked an iLIGO 10 W laser to a Lightwave NPRO and observed a long term drift of the free-running relative frequency between the two lasers (by monitoring the locking control signal) of less than 1 MHz per hour. However at low frequencies, the laser frequency is locked to the resonance length of the fused silica reference cavity. The thermal expansion coefficient of fused silica is about 5×10^{-7} 1/K, so the long-term temperature stability of the reference cavity would have to be better than 5 mK.

Measurements at Caltech are currently underway to measure the long term drift in the resonant frequency of a LIGO-style reference cavity system. It may be possible to achieve the required 5 mK stability even without thermal regulation of the temperature of the vacuum enclosure for the reference cavity. This would allow elimination of the temperature control loop including the high current DC power supply.

3.3 Control band frequency fluctuation levels

The allowed frequency fluctuations in the control band, from 0.1 to 10 Hz, are summarized in Table 3, below.

Frequency band	Frequency stability req.
1 – 10 Hz	< 3 Hz-rms
0.4 – 1 Hz	< 100 Hz-rms
0.1 – 0.4 Hz	< 1000 Hz-rms

Table 3. Allowed frequency fluctuations in the control band.

The iLIGO PSL performance with respect to these requirements has not been measured. It is expected to be dominated by the length fluctuations of the reference cavity. Again, the reference cavity measurements at Caltech, mentioned above, should enable estimation of the expected performance of the aLIGO PSL.

K. Numata et al. have analyzed the limits for frequency stabilization of a laser to a reference cavity[5]. They analyzed the best results achieved by J. Berquist at NIST and the A. Brillet group in France with a ULE cavity. Their results seem to indicate that the achievable stability is limited by the thermal noise in the mirrors contacted to the spacer. Even though there are no out-of-loop measurements between 1 Hz and 30 Hz available, a projection of the NIST and VIRGO results suggests that a frequency stability of about

[5]Kenji Numata, Amy Kemery, and Jordan Camp, *Thermal-Noise Limit in the Frequency Stabilization of Lasers with Rigid Cavities*, Phys. Rev. Lett. 93, 250602 (2004)

a factor of 100 better than the aLIGO requirements could be achieved. (Probably even better since the Q factor of fused silica is better than that of ULE).

3.4 GW band frequency noise levels

The required frequency noise levels in the GW band are shown by the blue lines in Figure 15, below. The iLIGO requirement is shown by the green lines. Note that above 100 Hz the aLIGO requirements have been relaxed by a factor of two and that they extend down to 10 Hz rather than 40 Hz, as for iLIGO.

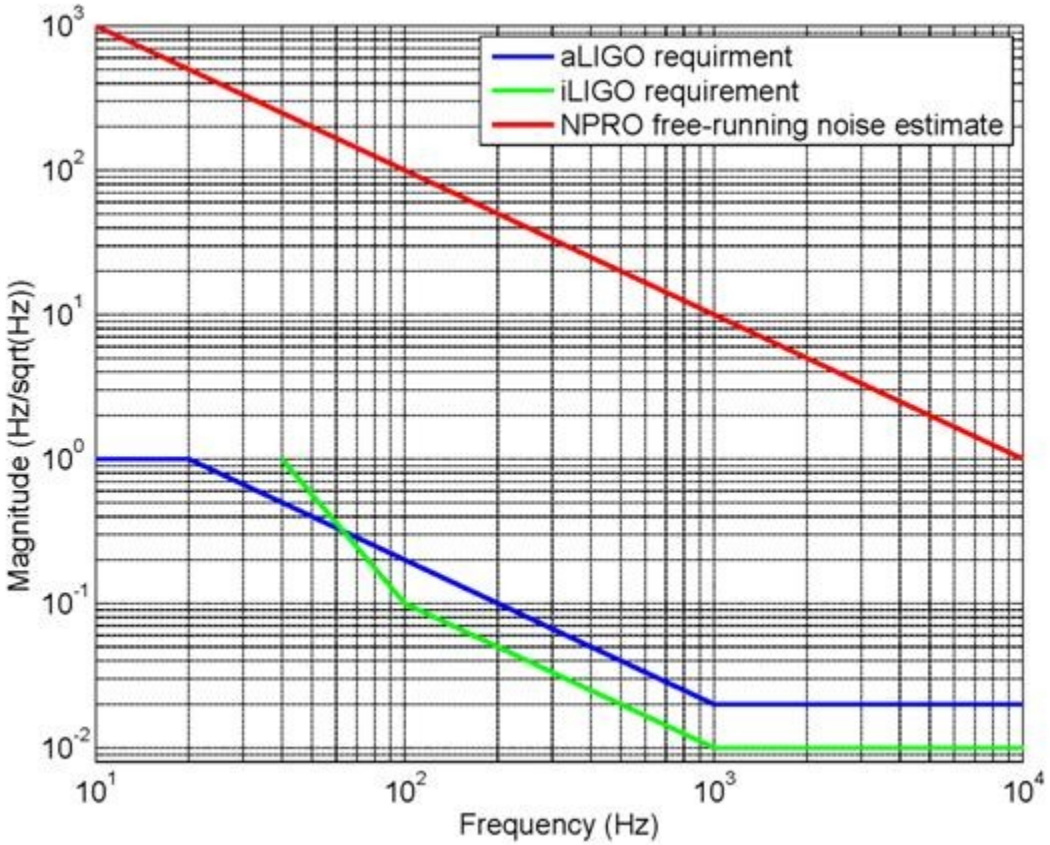

Figure 15. PSL free-running NPRO frequency noise estimate and *Advanced LIGO* and *Initial LIGO* frequency noise requirements.

The typical amplitude spectral density of the frequency noise of a free running NPRO can be approximated by 10 kHz / *f* Hz / √Hz, where *f* is the frequency of interest. This estimate of the free-running laser frequency noise is plotted in Figure 15 (red line). Figure 16 shows the measured the free-running frequency noise of the 200-W oscillator. It is less than 6 dB above the NPRO free-running noise estimate over the frequency range from 10 Hz to 10 kHz.

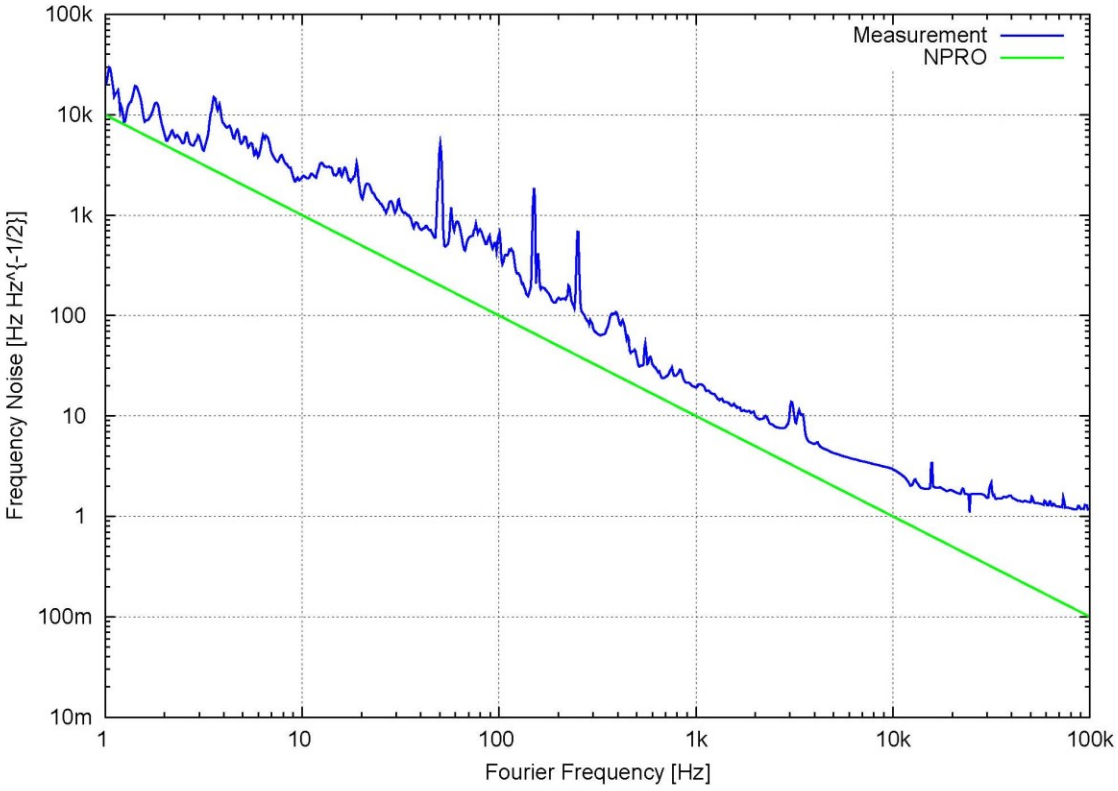

Figure 16 Measured free-running frequency noise of the 200-W oscillator. The frequency noise is about 5 dB above the noise estimate for the NPRO alone.

The open loop transfer function of the FSS operating in the LIGO H1 Interferometer[6] was measured in December, 2004 and is shown in Figure 17 (blue curve). Based on the estimate of the free-running frequency noise and the required suppressed frequency noise level (see Figure 15) we can estimate the required loop gain as shown by the green line in Figure 17. The measured loop gain exceeds the requirement by at least a factor of 10 (20 dB) at all frequencies up to 10 kHz and is above the required level of 20 dB at 100 kHz (see wideband frequency input requirements in Section 3.7).

[6] The FSS operating on the H1 system at the time of the measurements is referred to as the Table-top frequency stabilization servo (TTFSS). It is based on a revised FSS that is described in a document that can be found at http://www.ligo.caltech.edu/docs/T/T030076-00.pdf. The TTFSS servo electronics are located on the PSL table, close to the laser frequency actuators, and control and monitoring signals interface with the TTFSS module via an interface board situated in the Eurocard crate in the PSL electronics rack. The LIGO drawing numbers for the relevant electronics schematics are D040105 (Tabletop Frequency Stabilization Servo), D040423 (TTFSS Interface Board) and D040469 (RF Summing Box).

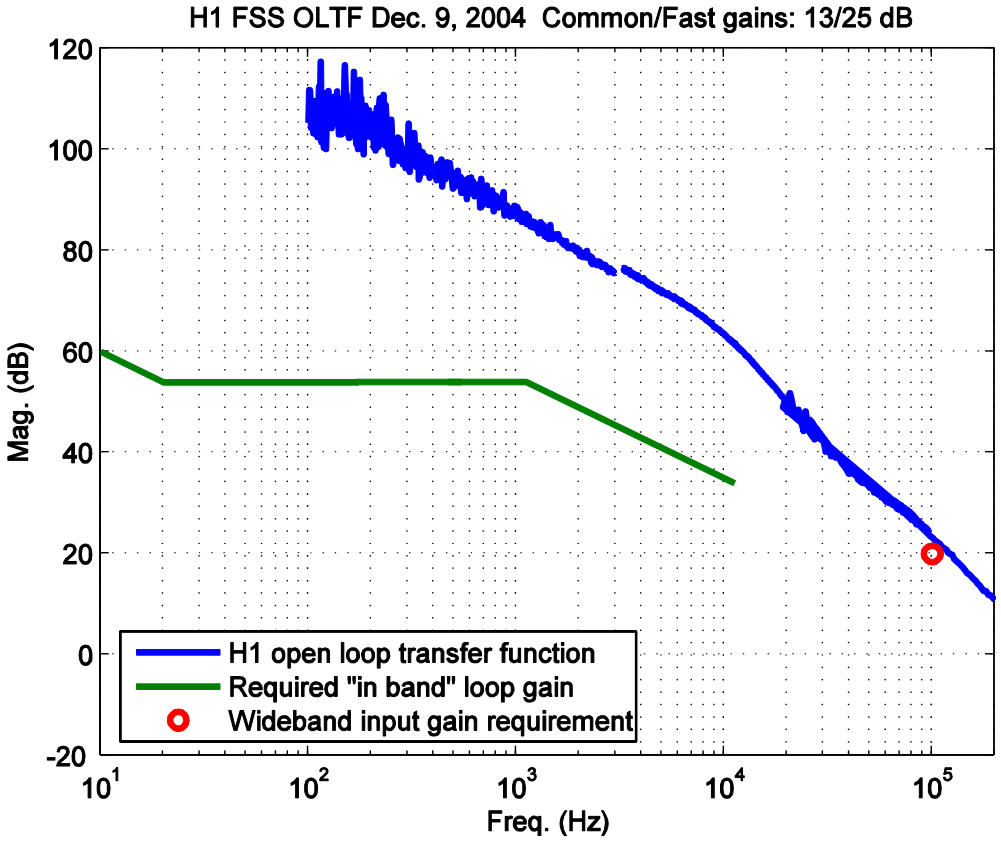

Figure 17. Measured iLIGO FSS open loop transfer function and gain required to meet the suppressed frequency noise requirement. For aLIGO 5 dB more loop gain is required.

3.5 iLIGO and eLIGO table-top frequency stabilization servo

The eLIGO PSL utilizes the TTFSS electronics which were used for iLIGO. The phase-correcting EOM for the eLIGO PSL is located inside the laser head, between the InnoLight Mephisto NPRO and the 35-W amplifier, rather than outside the MOPA as was the case for the iLIGO PSL. The actuation coefficient of the FAST actuator in the InnoLight NPRO is about a factor of five lower than for the Lightwave NPRO. The FAST path electronics gain was increased to compensate[7]. Figure 18 shows the FSS open loop transfer function measured with the H1 eLIGO PSL in April 2008. The

[7] Note that even with this modification the range at all frequencies is reduced due to the reduced actuation coefficient of the FAST actuator in the InnoLight NPRO. Instead of increasing the overall FAST path gain, we could have followed a suggestion by R. Adhikari and increased the frequency of the passive output pole in the FAST path, presently at 10 Hz, to 50 Hz. This would restore the range at frequencies above about 50 Hz where the range limit is imposed by the limited output voltage (~ ± 10 V) of the TTFSS electronics and the attenuation by the passive output pole. The gain below 10 Hz would still be 5× lower in this case.

performance is similar to that of the iLIGO PSL. It also exceeds the gain requirements for the FSS.

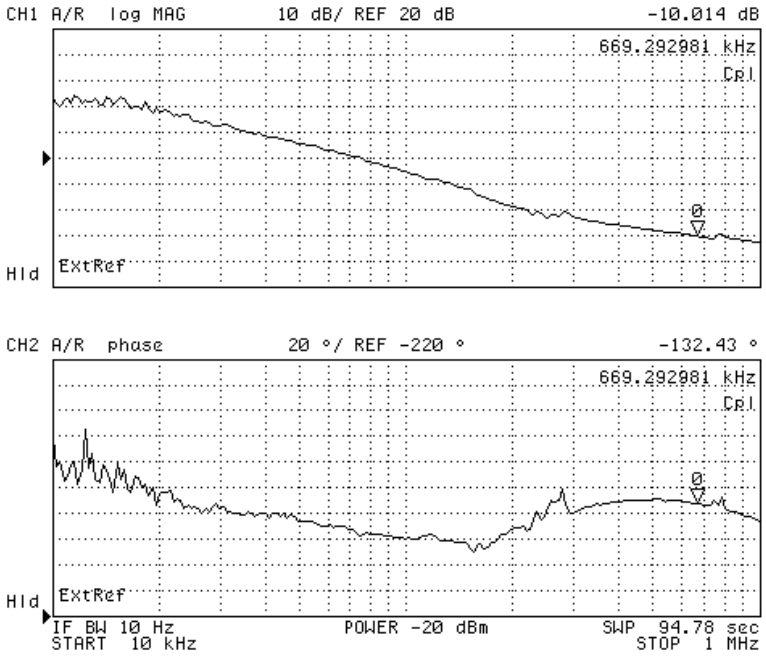

Figure 18. FSS open loop transfer function measured on April 18, 2008 with the H1 eLIGO PSL utilizing the LZH 35-W laser. Note that the unity gain frequency is at -10 dB. The loop gain at 100 kHz is about 5 dB more than the required 20 dB.

Figure 19 shows the LIGO H1 PSL frequency noise measured by the 15 m suspended modecleaner on October 2, 2004. This is an upper limit on the PSL frequency noise because it is the noise sensed by the modecleaner servo and includes modecleaner length and sensing noise as well as noise that might be added by the IO optical components between the PSL/IO interface point and the modecleaner. These include the three IO EOMs, the adjustable half wave plate and polarizing optics for power adjustment, and the IO periscope. The solid green lines represent the aLIGO PSL frequency noise requirements and the red lines are the iLIGO requirements. Note that except for a number of sharp peaks, which appear to be of acoustic origin, the iLIGO PSL meets the aLIGO PSL frequency noise requirements.

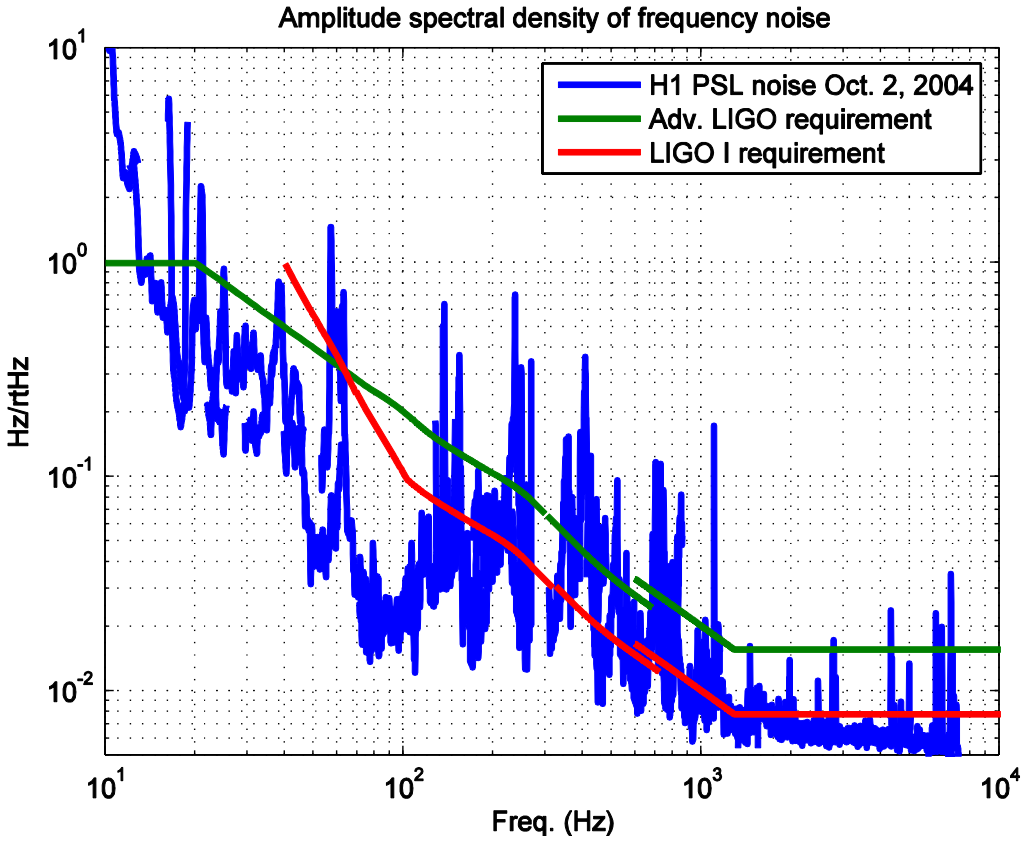

Figure 19. LIGO H1 PSL frequency noise performance measured by the 15-m-long suspended modecleaner on Oct. 2, 2004.

3.6 aLIGO table-top frequency stabilization servo

There are three significant differences between the eLIGO PSL and the planned aLIGO PSL that are likely to make the FSS work more challenging: i) the injection-locked high power oscillator is expected to add some phase delay due to the oscillator injection locking range; this is expected to be small, ii) because the FSS beam is sampled downstream of the PMC and the bandwidth of the aLIGO PMC (about 570 kHz) is significantly lower than the iLIGO PMCs (about 3.3 MHz) the PMC is expected to introduce about 45 deg of phase delay at 570 kHz, near the FSS loop unity gain frequency and about a 3 dB reduction in the frequency actuation of the phase-correcting Pockels cell if it is located upstream of the PMC, and iii) tens of nanoseconds of additional delay due to the increased optical path lengths and cable lengths due to the more widely distributed optical components.

A schematic diagram of the baseline aLIGO FSS scheme is shown in Figure 20.

-

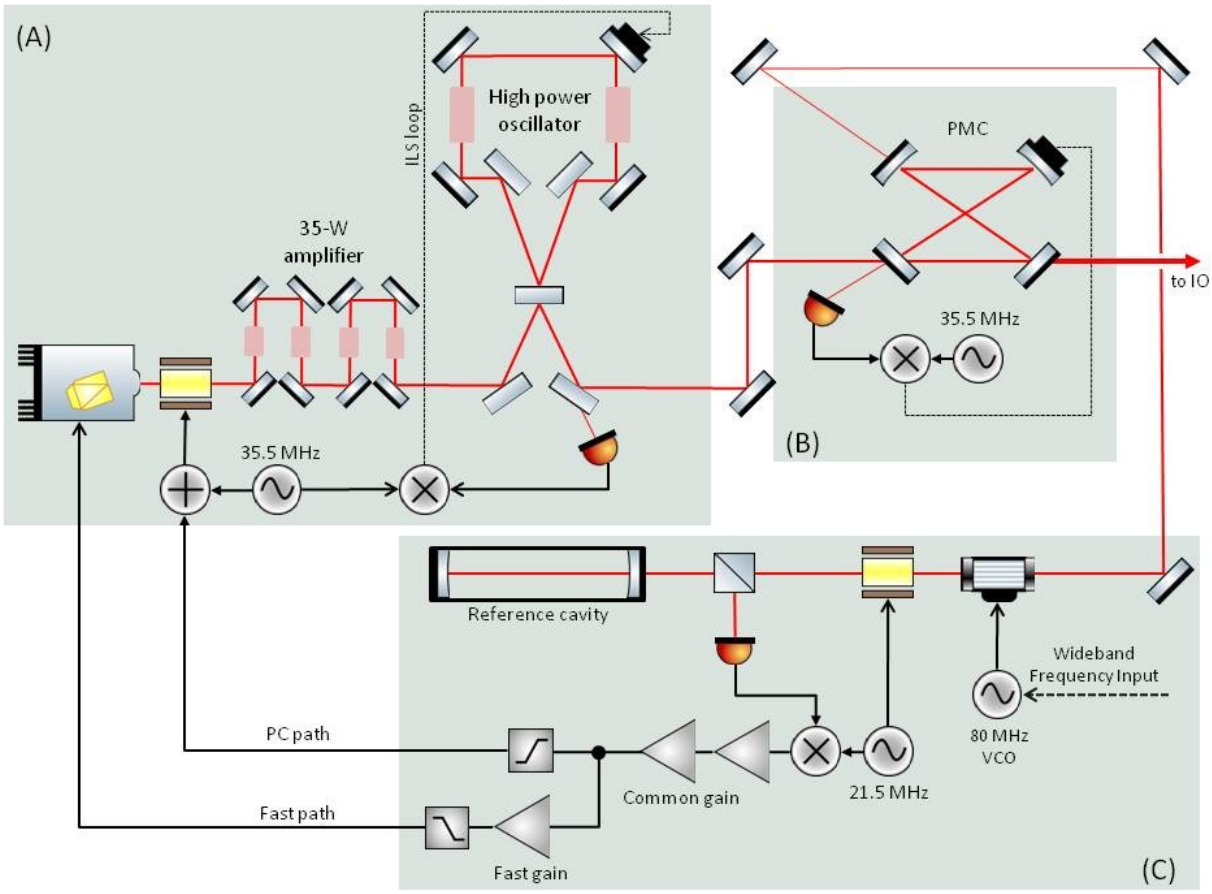

Figure 20. Schematic diagram of the frequency stabilization servo for the aLIGO PSL. Block (A) laser source including the injection locking loop, block (B) PMC its length control loop , and block (C) is the frequency stabilization loop. The output of the injection-locked high power oscillator is directed to the 4-mirror PMC which is in a bow-tie configuration and the circulating light transmitted through one of the PMC mirrors is used for the FSS loop. The SLOW actuator frequency control path is not shown in this diagram.

The beam for the FSS is sampled downstream of the PMC. It is directed to the frequency shifter on the way to the reference cavity, as for the eLIGO FSS. This scheme has the benefits that the beam directed to the FSS has been spatially filtered by the PMC and that frequency noise added by the PMC is suppressed by the FSS loop. However, because the PMC can introduce frequency changes as the length of the PMC is varied, the frequency control loop is coupled to the PMC length control loop. The error signal is generated by the usual PDH method with 21.5 MHz phase modulation sidebands (also as before) and conditioned by the TTFSS servo located on or near the

PSL/IO optical table before driving three frequency actuators: the SLOW actuator, which controls the NPRO crystal temperature, for frequencies below 1 Hz, the FAST actuator consisting of a PZT bonded to the NPRO crystal for strain-induced index of refraction changes at frequencies between 1 Hz and 20 kHz, and a phase-correcting EOM or Pockels cell for frequencies above 20 kHz.

With the aLIGO PSL layout, the optical path length from the phase-correcting Pockels cell, through the 35-W laser, the high power oscillator, and the PMC to the FSS RF photodiode is about 15 m and the cable from the RF photodiode to the TTFSS is about 5 m. These paths introduce time delays in the FSS loop. The PMC cavity and the high power oscillator cavity introduce phase delays and attenuation at higher frequencies due to the cavity poles. Therefore, the TTFSS electronics utilized for the iLIGO and eLIGO FSS loops, require modifications to increase the phase margin at the required unity gain frequency of 500-700 kHz. Efforts are underway to design, implement and test modifications to the TTFSS electronics that will enable achieving the required FSS performance in this configuration.

Figure 21 shows a measured open loop transfer function of the frequency stabilization loop with the PSL configuration shown in Figure 20 and with the eLIGO TTFSS electronics without making any modifications to increase the phase margin at high frequencies. The maximum unity gain frequency was about 80 kHz where the phase margin was only about 5 deg.

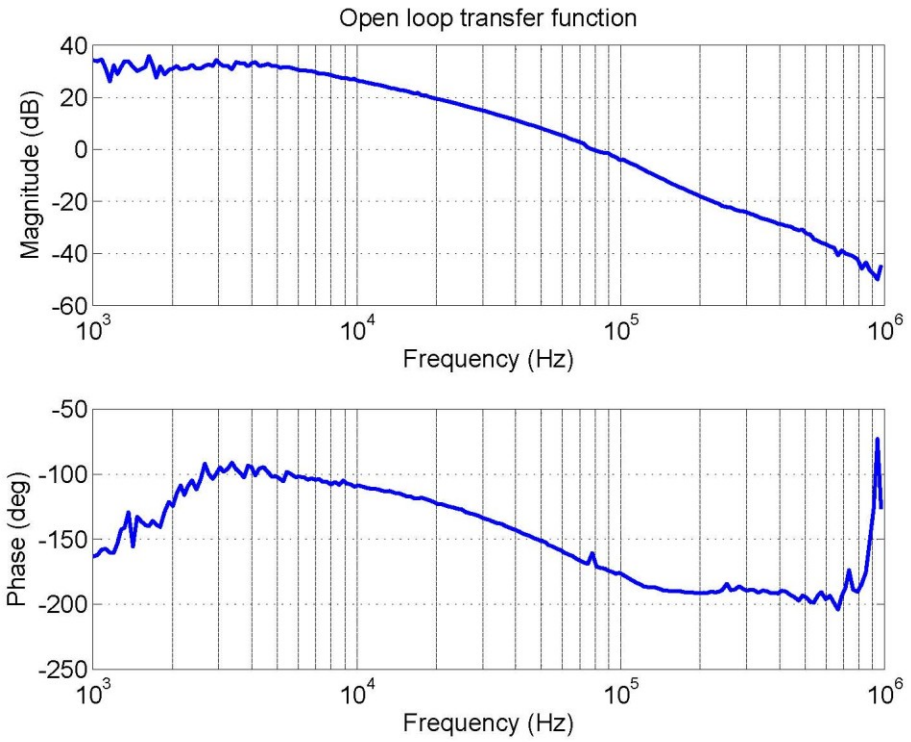

Figure 21. Measured open loop transfer function. The unity gain frequency is about 80 kHz with 5 degrees phase margin. Note that this

loop does not yet include a compensation circuit within the servo electronics.

As stated above, we think the main reasons for a lower control bandwidth compared with the eLIGO FSS are the PMC cavity pole and additional propagation delays (the corner frequency of the PMC is at about 570 kHz (refer to the PMC section), so we expect 45 degrees of phase delay at 570 kHz. The time delay due to the optical-path length from the Pockels cell to the FSS sensor is about 50 ns, and the time delay due to the cable from the sensor to the FSS servo is about 25 ns. It thus introduces about 15 degrees phase lag at 500 kHz.

To achieve a control bandwidth of 500 kHz to 700 kHz we will attempt to compensate for the PMC pole by adding a phase-lead compensation circuit to the FSS. With the baseline optical layout shown in Figure 20, the maximum unity gain frequency for the FSS loop was about 80 kHz (see Figure 21). In order to increase the phase margin at higher frequencies and achieve the require loop bandwidth, we have designed a modification to the FSS electronics. The phase compensation circuit schematic is shown in Figure 22. It adds a zero at 484 kHz, a pole at 3.4 MHz, and gain of 8 to the Pockels cell actuation path. Figure 23 shows the simulated open loop transfer function with (blue curves) and without (red curves) the phase-lead circuit. The simulations indicate we could achieve a unity gain frequency at 500 kHz with phase margin of 50 degrees. More importantly, it indicates that we could achieve the required 20 dB of gain at 100 kHz (see Section 3.7, below). The circuit has been fabricated on a daughter card and a test with the FSS was performed[8]. A unity gain frequency of 340 kHz with 30 degrees of phase margin and more than 18 dB of gain at 100 kHz was achieved. Further tests are ongoing.

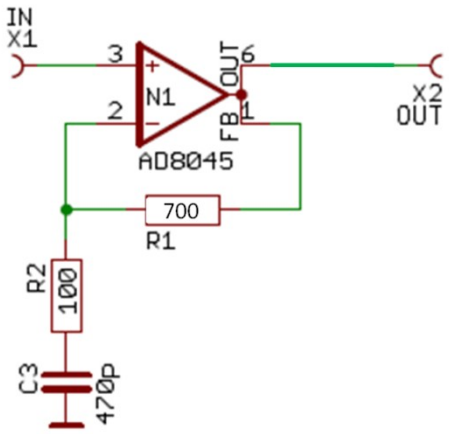

Figure 22. Phase-lead circuit to compensate for the responses of the high power oscillator, the PMC, and the propagation delay. It adds a zero at 484 kHz, a pole at 3.4 MHz and a factor of 8 gain.

[8] Please refer to Engineering Prototype Performance Document (LIGO T0900617-v1).

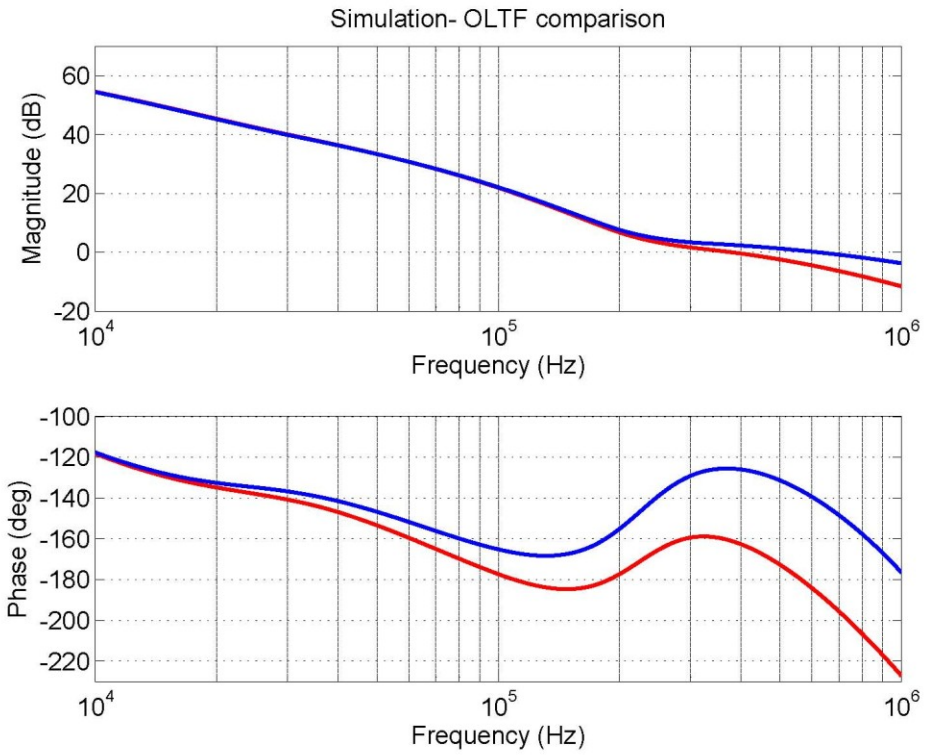

Figure 23. Simulated FSS open loop transfer function including PMC pole, high power oscillator pole, and time delay caused by the optical path length and the cable length. Blue curve: open loop transfer function with the compensation circuit, red curve: open loop transfer function without the compensation circuit.

A fall-back plan, in case the electronics modifications are untenable, is to use a phase-correcting Pockels cell located in the main beam downstream of the PMC and upstream of the FSS beam sample point as shown in Figure 24. This would circumvent the phase delays introduced by the injection-locked oscillator and the PMC.

This additional EOM would likely be very similar to the aLIGO 3-in-1 RTP modulator used by the IO subsystem, but with a single set of electrodes. The expected modulation index is 7 mrad/V (according to Volker Quetschke), about half of that for the New Focus modulator currently used. The wedge would likely be oriented opposite to the IO EOM to so that the induced beam deflections would cancel.

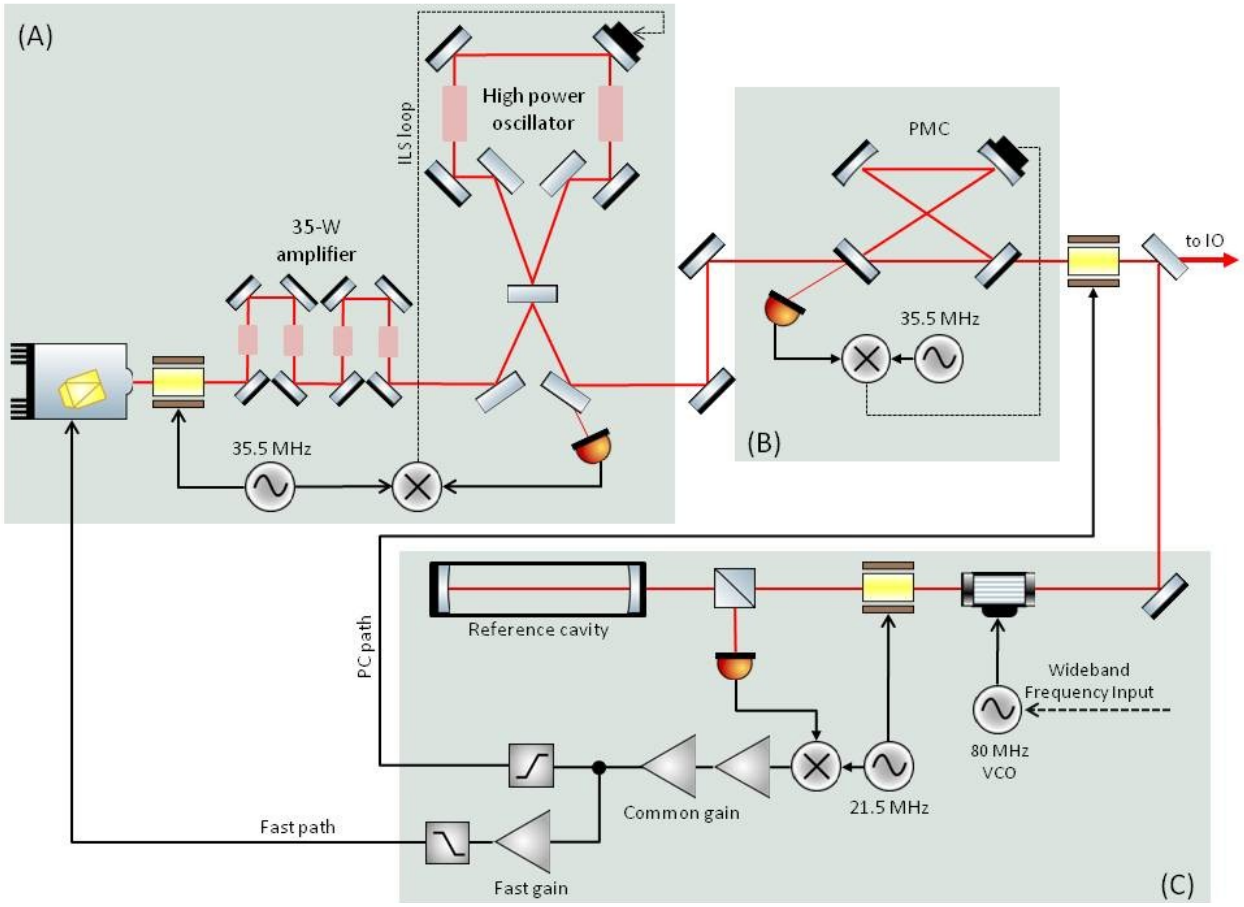

Figure 24. Schematic diagram of the fall-back FSS optical configuration with a high-power EOM similar to that used by the IO subsystem located downstream of the PMC. The SLOW actuator frequency control path is not shown in this diagram.

3.7 Wideband frequency input

The requirements for the *wideband frequency input* are summarized in Table 4, below.

Wideband frequency input	
Bandwidth	100 kHz: less than 20 degrees phase lag at 100 kHz
Range:	DC-1 Hz: 1 MHz pk-pk
	f > 1 Hz: 10 kHz pk-pk

Table 4. Wideband frequency input performance requirements.

As for iLIGO and eLIGO, the wideband frequency input is realized by a frequency shifter embedded in the FSS loop consisting of a double-passed acousto-optic modulator driven by a voltage controlled oscillator (VCO). The aLIGO requirements allow for a reduction in the VCO actuation range by a factor of ten compared with iLIGO. This reduced range allows for a reduction in the noise introduced by the VCO. The aLIGO PSL will utilize the aLIGO low-noise voltage controlled oscillator designed by D. Sigg. A detailed description of the aLIGO VCO can be found on the aLIGO wiki (see http://lhocds.ligo-wa.caltech.edu:8000/advligo/LowNoiseVco?highlight=(vco)).

The gain and phase lag requirement at 100 kHz translates into a required loop gain of at least 20 dB at 100 kHz for the frequency stabilization. As shown in Figure 18, the eLIGO TTFSS meets this requirement.

3.8 Tidal frequency input

The requirements for the *tidal frequency input* are given in Table 5.

Range: 50 MHz pk-pk
Speed: time constant < 5 hrs.

Table 5. *Tidal frequency input* performance requirements.

Given the large range of the SEI subsystem's hydraulic actuators, the tidal effects will most likely be compensated for by a simple correction of the arm lengths at all frequencies (rather than having the laser frequency follow the arms at tidal frequencies). However, because a slow frequency control input might be useful for other purposes, the tidal input will be maintained as an option.

The hardware and electronics for the aLIGO *tidal frequency actuator* are identical to those utilized for iLIGO. Frequency changes are realized by changing the temperature of the reference cavity to which the laser frequency is locked. The temperature of the reference cavity is varied via changes in the temperature of the stainless steel vacuum chamber in which the reference cavity is suspended.

At Hanford, a computer model is used to predict the tidal stretching along the interferometer arms. This model, together with empirical estimates of the response of the reference cavity to changes in the temperature of the vacuum enclosure, is used to generate a time series of predicted vacuum chamber temperatures. With the predicted temperatures fed to the reference cavity vacuum chamber temperature controller, long lock stretches enable determination of the degree of tidal compensation achieved. This is accomplished by monitoring the residual drive to the end test mass fine actuators required to relieve the drive on the suspension controllers.

The common and differential tidal predictions and the residual length corrections required after the predicted correction has been applied to the *tidal frequency input* are shown in Figure 25. Note that the residual common mode tidal effect has been reduced by about a factor of four, from roughly 90 μm p-p to about 20 μm p-p.

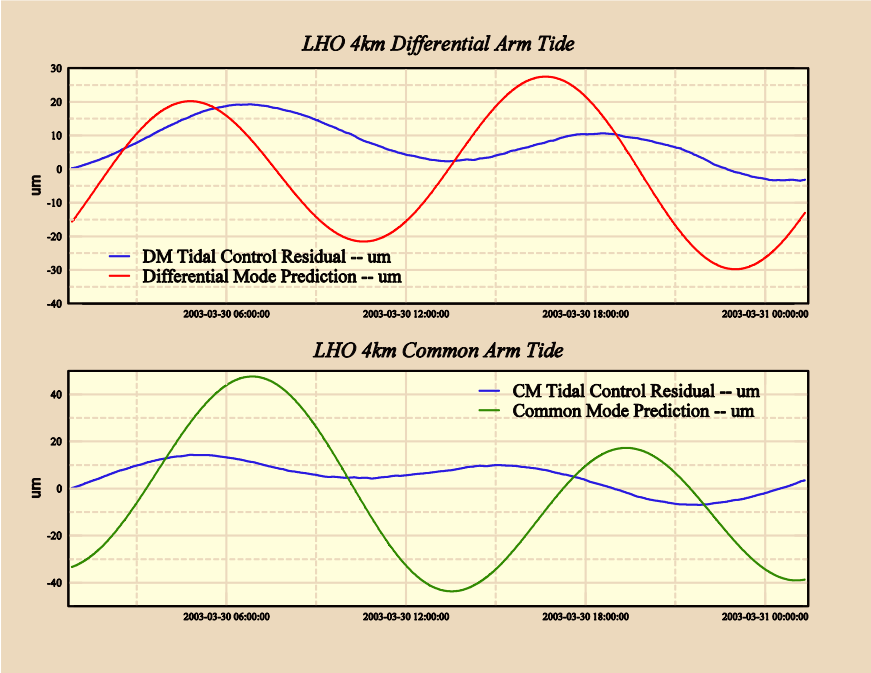

Figure 25. Performance of the LIGO H1 tidal compensation system.

4 Pre-Modecleaner

The pre-modecleaner (PMC) is responsible for spatial filtering and the suppression of power fluctuations at radio frequencies. Due to a new requirement for relative power noise at radio frequencies (RPN-rf) it was necessary to design a new PMC for Advanced LIGO (see Section 4.1). It is put into the main beam path and has a high transmission for the fundamental mode. A length control system consisting of two actuators is used in order to keep the circulating light field resonant with respect to the incoming beam (see Section 4.2). The PMC is housed inside a sealed tank, which provides acoustic shielding, is a thermal enclosure and is dust-free. A first prototype was assembled and tested with high power (see Section 4.3) at the AEI.

4.1 Design

The PMC consists of four mirrors mounted to an aluminum spacer (see Figure 27) arranged in a bow tie configuration with an edge length of 0.5 m. There are two curved and two flat mirrors mounted onto the spacer (see Table 6). The flat ones are used as input and output coupling mirrors for the high power beam. The fraction of the circulating light transmitted through the curved mirrors is used for further analysis and stabilization.

Compared to the iLIGO PMC the finesse is reduced to 130 in order to have a good tradeoff between a reduction of RPN-rf to meet the requirement and a suitable

amount of circulating light power. The upper limit for the peak intensity at the mirror surfaces was set such that it does not exceed 1.5×10^6 W/cm^2. At this intensity long term tests with another PMC showed no beam distortions due to absorption.

finesse	130
round trip length	2.02 m
FWHM	1.15 MHz
transmission of flat mirrors	2.4%
transmission of curved mirrors	65 ppm
suppression factor of transmitted power in TEM_{01} and TEM_{10}	4000
waist of beam between flat mirrors	550 μm
waist of beam between curved mirrors	710 μm
actuator range of PZT	2.7 FSR for 0–375 V
actuator range of thermal actuator	5 K
bandwidth of PZT control loop	10.5 kHz
thermal control loop	time constant of 3 hours
size of the tank (h×w×d)	150 mm × 590 mm × 250 mm

Table 6. Properties of PMC and its control loops.

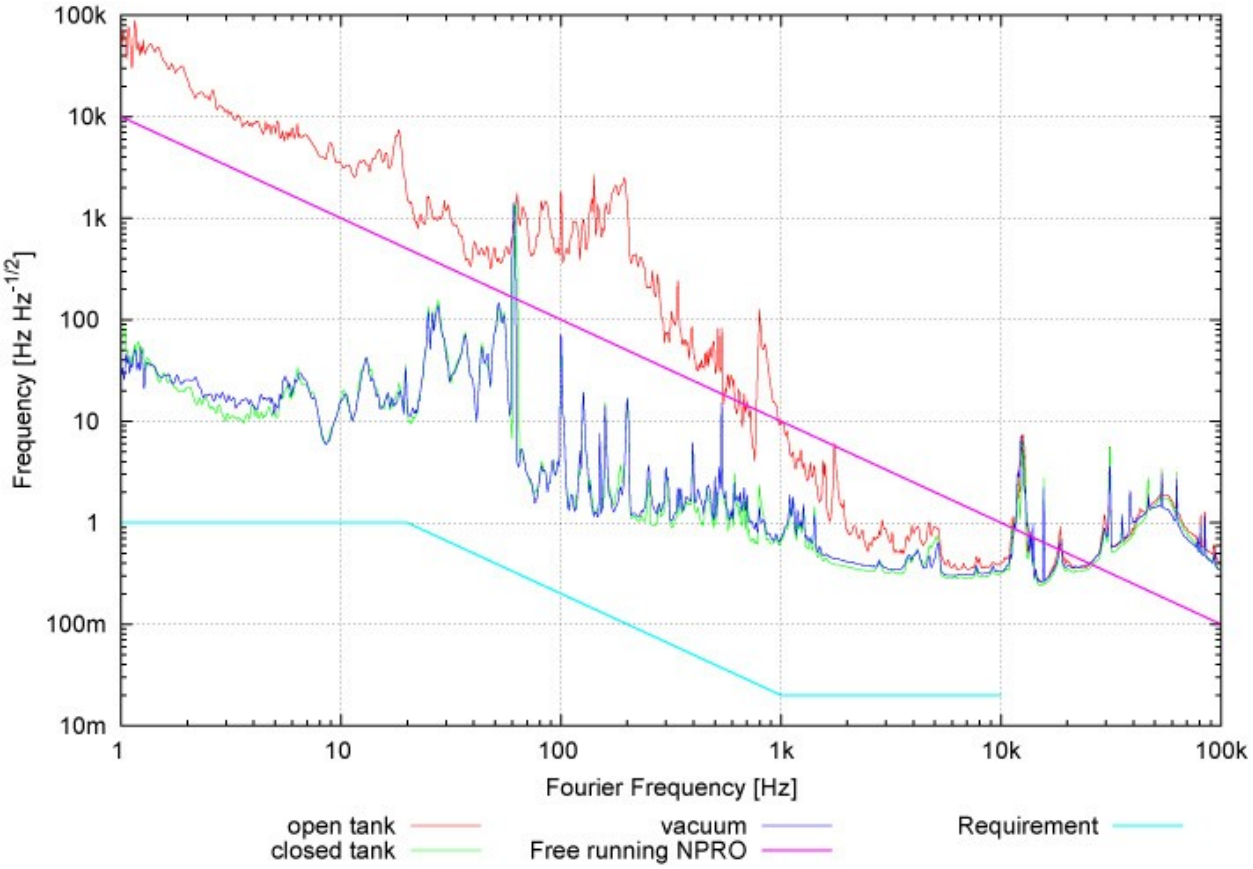

Figure 26. Equivalent frequency noise of a PMC prototype (DBB style) which was placed into a vacuum chamber. For this measurement a NPRO was stabilized to a high finesse reference cavity. Different measurements are shown with a open tank, a closed tank and an evacuated tank. The free running noise of a NPRO and the PSL frequency noise requirements are shown as a reference.

The PMC is assembled in a cleanroom in order to keep any dust particles away from the mirrors and from the spacer. To avoid acoustically driven length changes of the PMC and to keep the PMC mirrors clean and its transmission high, the PMC is put into a sealed vessel. According to investigations at the AEI the placement in a sealed container can reduce the effective length fluctuations by about two orders of magnitude (see Figure 26) to a level well below the equivalent free running noise of the NPRO. No further improvement could be achieved by evacuating the tank. However, it is not good enough as reference cavity.

4.2 Length control system

For the length control of the PMC two actuators are used, a PZT glued between the spacer and one of the curved mirrors to compensate for fast deviations from the

resonance and secondly two thermal pads which heat up the spacer in order to keep its length constant. The locking is done with a Pound-Drever-Hall locking scheme and sidebands at 35.5 MHz that are produced by the EOM in the 35 W Front End laser.

The Pound-Drever-Hall locking requires an external rf source with an optimized demodulation phase. The PMC electronics provides an automated locking function which compares the dc signal of the locking PD with a reference value and steers a ramp generator such that the ramp is turned off when the PMC is on a resonance and the loop is able to keep the system in a locked state (see Figure 27). When lock is lost the ramp is automatically switched engaged. A high voltage operational amplifier converts the control signal to a voltage level where the PZT can operate.[9,10]

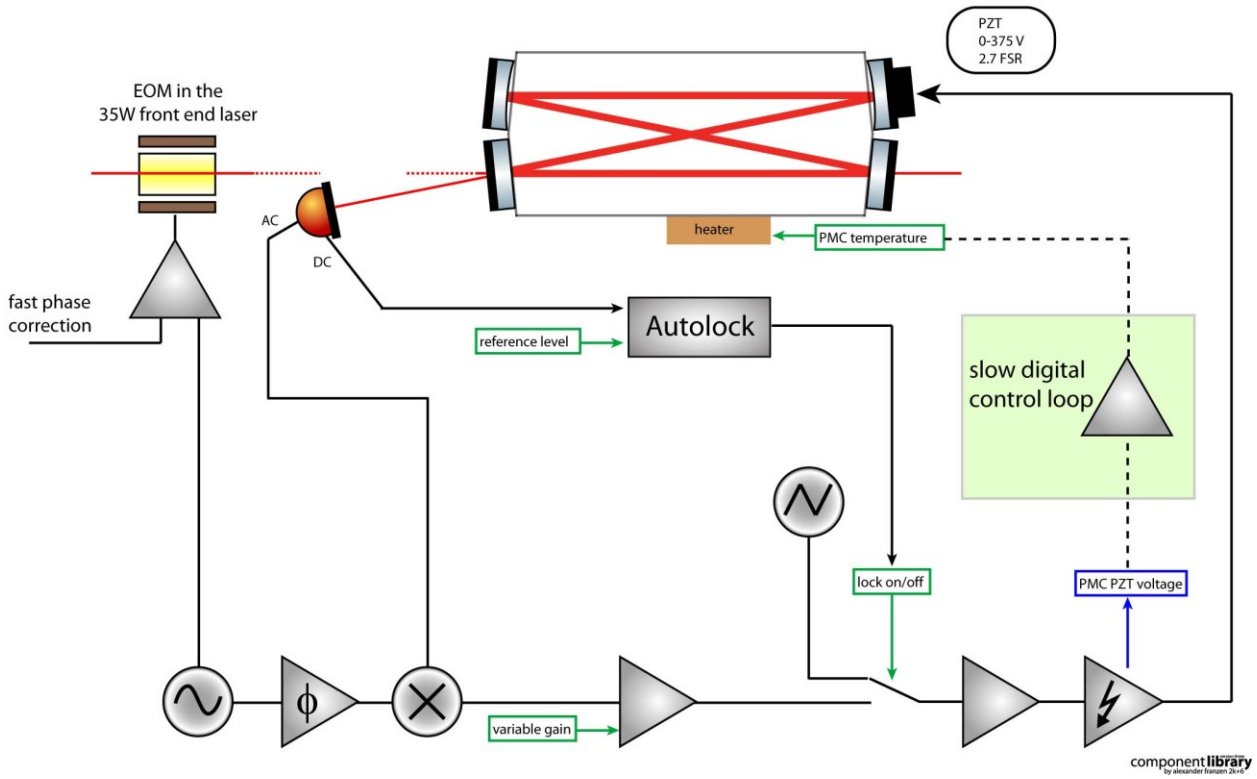

Figure 27. Schematic of the length control system with an automatic lock acquisition and a temperature control for the PMC to keep the optical path length constant.

The thermal actuator is digitally controlled via EPICS. This control loop takes care that the PZT voltage always stays in the middle of the range. Thus it was possible to operate the PMC without any relock whilst the room temperature was changed by 2.5 K.

---

[9] Patrick Kwee, "Advanced LIGO PSL injection locking and PMC locking electronics – circuit board documentation" (LIGO T0900577-v1).

[10] Patrick Kwee, "Advanced LIGO PSL injection locking and PMC locking electronics – function and interface document". (LIGO T0900578-v1).

4.3 Performance

With the power stabilization engaged it is possible to deliver more than 160 W through the PMC. The locking of the PMC is stable over more than 48 hours and the higher order mode content downstream of the PMC is well below 5%. More detailed information about the measurements presented in this section can be found in the Engineering Prototype performance document[11]. The results and assumptions shown in the following all fit within the acceptable tolerances identified during the design phase of the PMC[12].

In the eigenbasis of the PMC, pointing can be interpreted to first approximation as an excitation of first order TEM modes[13]. Since these modes are not resonant the PMC suppresses the pointing by a factor of 63. The graph in Figure 28 shows the worst pointing noise curve measured with the DBB downstream from the high power oscillator and the latter curve is projected to a level that was calculated by the attenuation factor. This represents the relative pointing noise at the output of the PMC and indicates that the aLIGO requirement will be met.

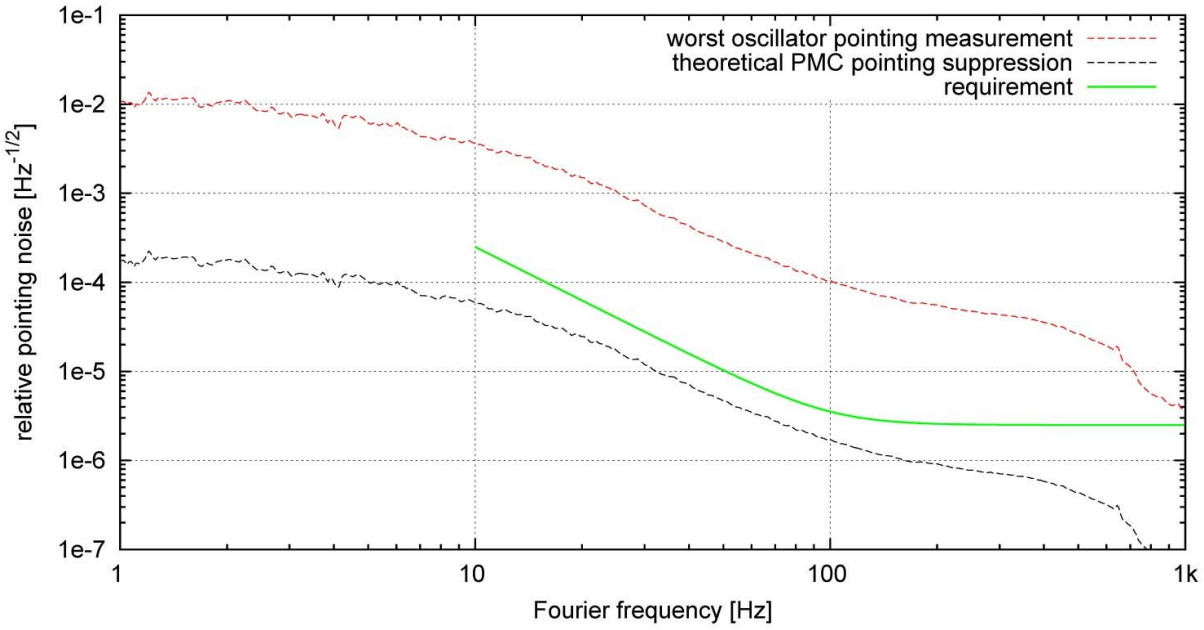

Figure 28. Relative pointing noise of the oscillator with a theoretical model for the pointing suppression of the PMC.

The dominant source for RPN-rf is the NPRO power noise. The new aLIGO requirement (in force since the aLIGO PSL preliminary design review) is: a maximum

[11] Jan Pöld, Engineering Prototype Performance document (LIGO T0900617-v1).

[12] Jan Pöld, aLIGO bow-tie Pre-Mode Cleaner document (LIGO T0900616-v1).

[13] P. Kwee, F. Seifert, B. Willke and K. Danzmann, "Laser beam quality and pointing measurement with an optical resonator". Review of Scientific Instruments. 2007

power noise of 1 dB above shot noise of 100 mA photo current at frequencies of 9 MHz and above.[14]

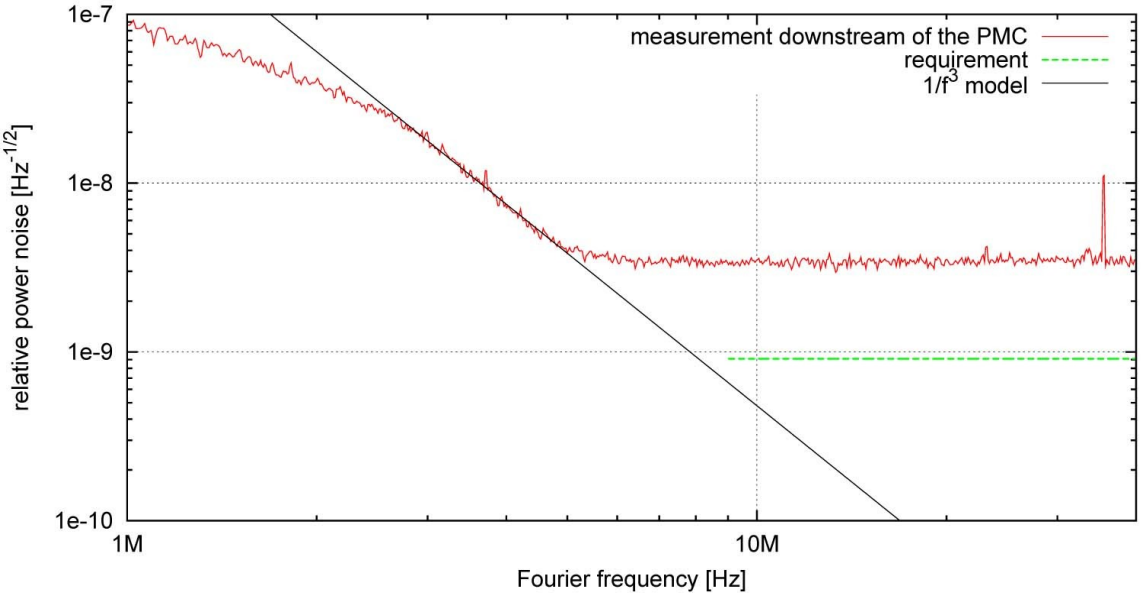

Figure 29. Relative power noise at radio frequencies. The measurement is shot noise limited above 5MHz. To simulate the RPN-rf for higher frequencies an f^{-3} model is assumed.

The shot noise level of the available photodiode was too high to demodulate the new requirements. However, we can assume in the low pass approximation that the filter effect of the power fluctuations provided by the PMC is proportional to f^{-1} in this frequency range.

The technical noise of the high power laser is dominated by the relaxation oscillation of the NPRO at 1 MHz[15]. At radio frequencies the technical noise decreases proportional to f^{-2}. As shown in Figure 29 the power noise downstream of the PMC falls with f^{-3} according to the combination of PMC filtering and the behavior of the technical noise of the NPRO. The assumed model demonstrates that the technical noise at 9 MHz is below the requirements.

5 Power Stabilization

The most demanding PSL requirement is the power stability of 2×10^{-9} $1/\sqrt{\text{Hz}}$ at 10 Hz at a location after the suspended input modecleaner. To achieve this goal, a nested loop with two sensing photodetectors and an acousto-optic modulator is used. The first photodetector senses the light transmitted through the concave mirror of the PMC and

[14] Benno Willke, Peter King, Rick Savage, Peter Fritschel, "Pre-Stabilized Laser Design Requirements" (LIGO T050036-v1).

[15] P. Kwee and B. Willke, "Automatic laser beam characterization of monolithic Nd:YAG nonplanar ring lasers." Optical Letters. 2008.

the second photodetector senses the light in a beam sampled after the suspended input modecleaner. A sketch of the power stabilization scheme is shown in Figure 30.

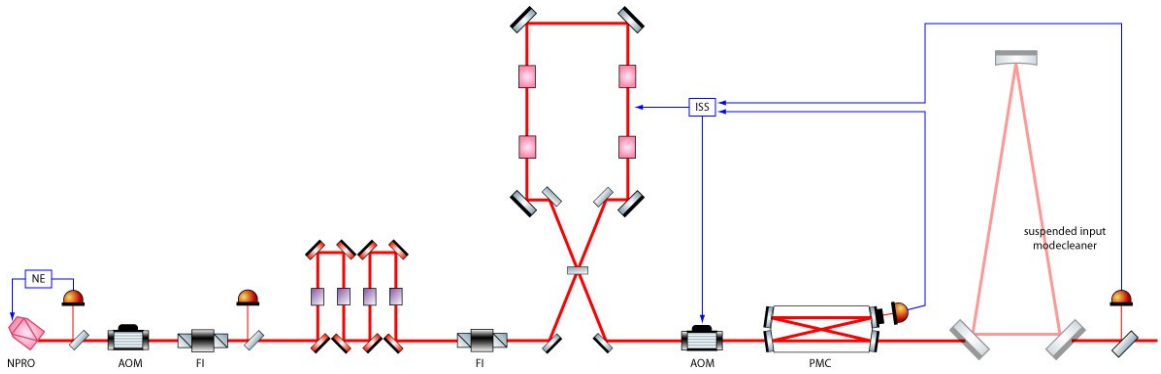

Figure 30. The power stabilization scheme.

The first loop is internal to the Mephisto master oscillator and is used to reduce the relaxation oscillation of the laser at ~1.2 MHz. The second control loop, called the inner loop, is DC coupled and actuates on the acousto-optic modulator located outside the aLIGO Laser. The third loop, called the outer loop, senses the power fluctuations after the suspended input modecleaner and will feed back into the error point of the inner loop.

Recently the power stability requirement was demonstrated with an NPRO at the AEI[16] using an electro-optic modulator as the power actuator and a photodiode array as the high power photodetector. The experiment was performed in a sealed container that was vented with HEPA filtered air to minimize the number of dust particles potentially traversing the beam path. Care was taken to minimize the effects of beam jitter on the power noise sensed by the photodetector . Another point to note was that the intensity stabilization electronics for the experiment were located in air.

5.1 Low Frequency Power Variations

The requirement for low frequency power stability is that the power fluctuations should be less than 5% peak-to-peak over any 24-hour period without intervention. In addition, there is a requirement that there be an input to the PSL that would enable power stabilisation at sensing ports in the interferometer to a level of 1% peak-to-peak for time scales longer than 10 s to 24 hours.

A long term measurement of the power fluctuations of the Engineering Prototype over a period of 12 hours is shown in Figure 31. The maximum fluctuation observed was 6% peak-to-peak, most of the fluctuations were within the 5% peak-to-peak range.

[16] Patrick Kwee, Benno Willke and Karsten Danzmann. “Shot-noise-limited power stabilization with a high power photodiode array” (Optics Letters, 34, 2912 (2009)).

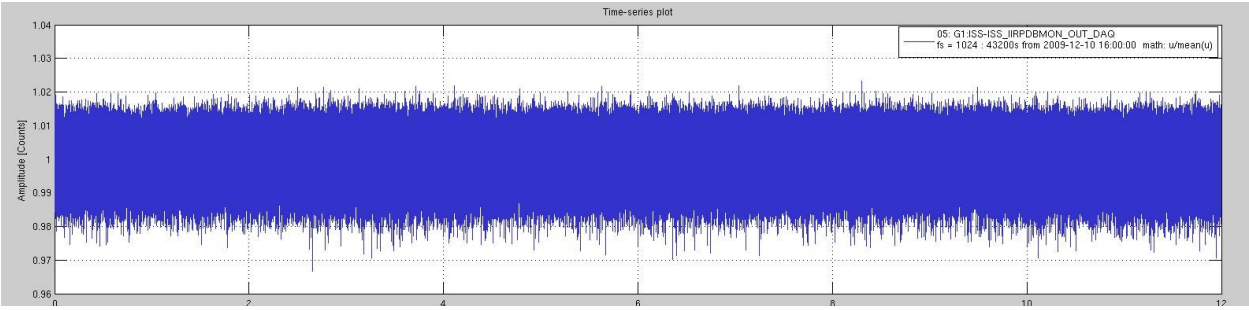

Figure 31. The power fluctuations of the Engineering Prototype laser measured over 12 hours.

5.2 Control Band Fluctuations

The control band is defined as the frequency range from 0.1 to 10 Hz. The relative power noise requirements in this band are summarised in Table 7[17].

Frequency [Hz]	$\delta P_{\mathrm{rms}}/_{P}$ [1/√Hz]
0.1 to 0.2	10^{-2}
0.2 to 0.5	$10^{-2}\left(\frac{f}{0.2}\right)^{-6.78}$
0.5 to 10	$2\times 10^{-5}\left(\frac{f}{0.5}\right)^{-3.07}$

Table 7. The relative power noise requirements in the control band.

The free running noise of the functional prototype was measured over 300 s (see Figure 32). From this time series we estimate the control band power noise to be below 10% peak-to-peak. A noise spectrum indicates that most of the power noise is at frequencies below 100 Hz.

[17] Pre-Stabilized Laser Design Requirements (LIGO T050036-v2), Section 2.2.

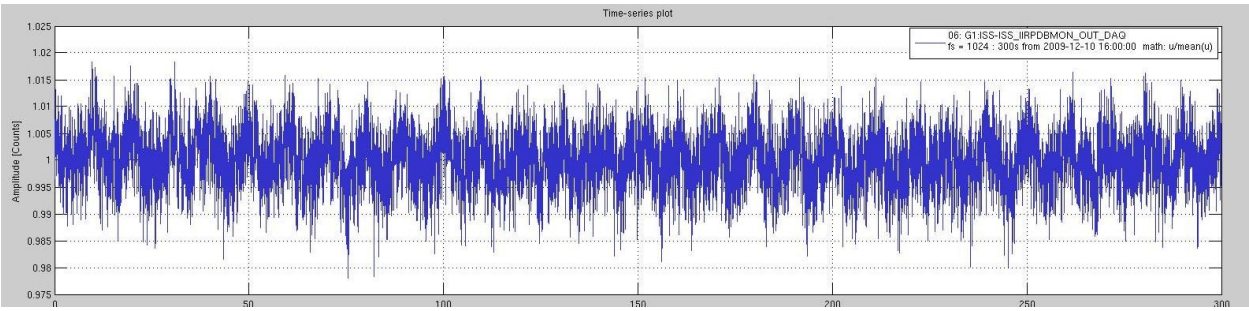

Figure 32. The free-running power noise of the functional prototype measured over 300 seconds. The maximum peak to peak variation is 4%.

5.3 Fractional Power Fluctuations in the GW Band

The power noise requirement is summarized in Table 8.

Frequency [Hz]	**Requirement** [1/√Hz]
10	2×10^{-9}
$10 < f < 100$	$2 \times 10^{-10}\ (f/\mathrm{Hz})$
$100 < f < 1000$	2×10^{-8}
$1000 < f < 10000$	$2 \times 10^{-11}\ (f/\mathrm{Hz})$

Table 8. The aLIGO PSL relative power noise requirements.

5.4 Photodiodes

In the Preliminary Design, the 3mm InGaAs PD3M photodiode from Gtran was identified as being suitable for the power stabilisation. Subsequent dark current noise and quantum efficiency measurements for a larger sample of PD3M photodiodes have determined that the PD3M does not meet the requirements for power stabilization.

An alternative is the PerkinElmer 2 mm InGaAs C30642GH photodiode and the 3 mm InGaAs C30665GH photodiode. Both these photodiodes meet the power stabilisation dark current noise requirements. 3 mm photodiodes will be used for the high power photodetector. This eases some requirements for the beam pointing control onto the photodetector. It should be noted that the power stabilization experiment was performed on an NPRO at the AEI and used 2 mm photodiodes.

5.5 Power Stabilization After the Suspended Input Modecleaner

In mid-2009, SYS advised that the outer loop power stabilization would be reviewed at a later date closer to the time when the power stabilization is required by the interferometer. The plan is to use the in-vacuum photodetector currently being designed by ISC, if it meets the requirements for the power stabilization, and interface it

to the power stabilization servo provided by the AEI. The final decision regarding the outer loop power stabilization will be reviewed elsewhere.

The following sections describe the considerations for the power stabilization photodetector.

5.6 Beam Jitter

Numerous laboratory bench top experiments have highlighted the effects of beam jitter on the sensing photodetector used in power stabilization. For the photodetector located after the suspended modecleaner, two sources of beam jitter are considered:

- Beam jitter due to motion of the HAM table
- Beam jitter from the suspended input modecleaner

The beam pointing requirements for the photodetector are plotted in Figure 33.

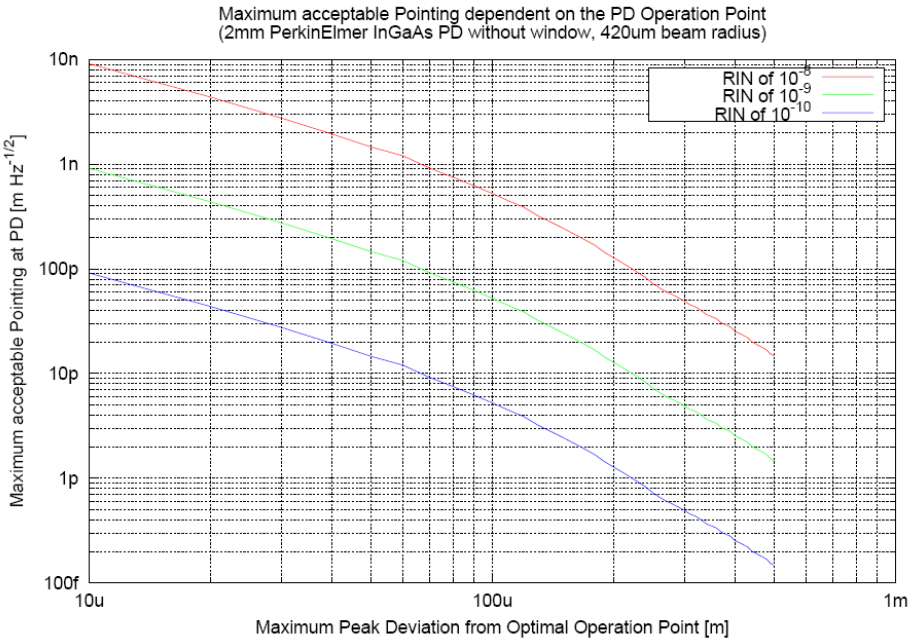

Figure 33. Pointing requirements for the power stabilization photodetector.

5.6.1 Beam Jitter Due To Motion of the HAM Table

The HAM table has a displacement limit of 4×10^{-11} m/√Hz.[18] This limits the DC alignment deviation from the photodetector's sweet spot to be a maximum of ~110 μm.[19] Controlling the beam jitter to this level is not difficult and simply requires a beam pointing control system consisting of a quadrant photodetector and steering mirrors.

[18] Peter Fritschel, "HAM Seismic Isolation Requirements (LIGO T060075-00-D)".

[19] Patrick Kwee, "Pointing Requirements at the Power Stabilization Photodiode behind the Mode Cleaner (LIGO T0900132-v1)".

Assuming that the peak-to-peak motion of the suspended input modecleaner will not exceed 100 μm, the photodetector will not be suspended.

5.7 PSL Beam Jitter From the Suspended Input Modecleaner

The beam jitter into the suspended input modecleaner, for frequencies less than 100 Hz, is given by[20]

$$a_{10}(f) < 2.5 \times 10^{-4} \left(\frac{10}{f}\right)^2 \quad \frac{1}{\sqrt{\text{Hz}}}$$

Applying the suspended input modecleaner's filtering factor of 250, the beam jitter out of the suspended input modecleaner is then

$$a_{10}(f) < 1 \times 10^{-6} \left(\frac{10}{f}\right)^2 \quad \frac{1}{\sqrt{\text{Hz}}}$$

Thus at 10 Hz, $a_{10} = 1 \times 10^{-6}\ 1/\sqrt{\text{Hz}}$. For a ~840 μm diameter beam on the surface of the photodetector, this would result in a beam pointing of 0.42 nm/√Hz. The maximum acceptable peak deviation from the photodetector sweet spot is then 18 μm. Controlling the beam position on the photodetector to this level will require a beam pointing control system.

IO will provide the beam steering actuators to position the beam onto the photodetector. At the time of writing this document, the tip-tilt stages used elsewhere in the interferometer were proposed by IO to fulfill this function. A quadrant photodetector will be used for the alignment of and sensing of the position of the beam on the high power photodetector.

6 PSL Internal Diagnostics

Several photodetectors, CCD cameras and diagnostic instruments are used to continuously monitor the performance of the different laser stages and the stabilizations and to assist identifying and solving problems concerning the PSL. Many laser internal diagnostic signals are acquired by the laser computer and are available as EPICS channels. These laser internal signals are not the scope of this section and a list of all laser channels available in EPICS can be found in the interface document (aLIGO PSL interface document LIGO T0900644-v1).

6.1 Laser Beam Diagnostics

The main diagnostic instrument for characterizing the beam of the 200 W and 35 W Front End is the diagnostic breadboard (DBB). The DBB is a compact, standalone diagnostic unit for laser beams. The relative power noise between 1 Hz and 100 kHz and between 1MHz and 100 MHz, the frequency noise between 1 Hz and 100 kHz, the pointing between 1 Hz and 100 kHz and the spatial beam quality of the incoming beam can be measured. These measurements can be performed locally using a function generator, an oscilloscope and a spectrum analyzer and may also be performed

[20] Guido Mueller, "Pointing requirements for Advanced LIGO (LIGO T0900142-v2)".

remotely using the aLIGO CDS system. The instrument is described in the DBB instruction manual (LIGO T0900133) and the interface to CDS is described in the DBB computer control manual (LIGO T0900579).

In the following the characterization and measurement methods of the DBB are summarized. An optical layout of the DBB is shown in Figure 34. The relative power noise is measured with an InGaAs photodiode with 50 mA photocurrent. Signal conditioning is done in the readout electronics of the photodiode. The frequency noise is measured with a ring resonator with a finesse of 360 and the Pound-Drever-Hall technique. The resonator is locked to the fundamental mode and the error signal and the control signal of this feedback loop is used to measure the frequency noise. The resonator is placed in a chamber for acoustic shielding. The alignment as well as the mode matching can be adjusted remotely. The pointing is measured using the differential wavefront sensing (DWS) technique and the same resonator. Two quadrant photodiodes are used to generate the DWS signals. Four alignment loops are used to automatically align the incoming beam to the resonator. The error signals and the control signals are used to measure the pointing of the incoming beam. The beam quality is measured using the modescan technique and the resonator. The transmitted power is measured with a low offset photodiode whilst the ring resonator is scanned. The higher mode content can then be calculated from the photodiode signal with a special computer program. The DBB is controlled in a fully automated mode by the PSL computer (EPICS/RTLinux) such that regular diagnostic runs can be performed during detector commissioning and during maintenance intervals in science runs.

A fraction of the 35 W beam as well as a fraction of the 200 W beam picked off in front of the PMC can be directed into the DBB for an analysis of the 35 W beam and the 200 W beam. Two shutters (Shutter1 and Shutter2[21]) are used to select the input beam for the DBB. In general the DBB can operate with an input power level between 120 mW and 150 mW.

Besides the DBB, two CCD cameras (CCD1 and CCD2) are used to monitor the transversal beam profile of the 35 W and high power laser beam. The pick offs will be in the beam paths towards the DBB. These video signals will be provided for display in the observatory control room.

Furthermore the average power and the power noise of the 35 W beam and the 200 W beam are monitored with a photodetector (PD1 and PD7), which is connected to CDS. A photodetector (FE_NPROMONITOR) between the NPRO and 35W amplifier is used to monitor the average power and the power noise of the NPRO. In addition this photodetector contains a trigger for the NPRO relaxation oscillation at about 1 MHz. This digital trigger signal is connected to CDS.

[21] For abbreviations such as Shutter1, Shutter2, CCD1, CCD2, PD1 ... etc, please see Figure 2. For a high resolution version of Figure 2, please see PSL/IO table layout (LIGO T0900610-v1).

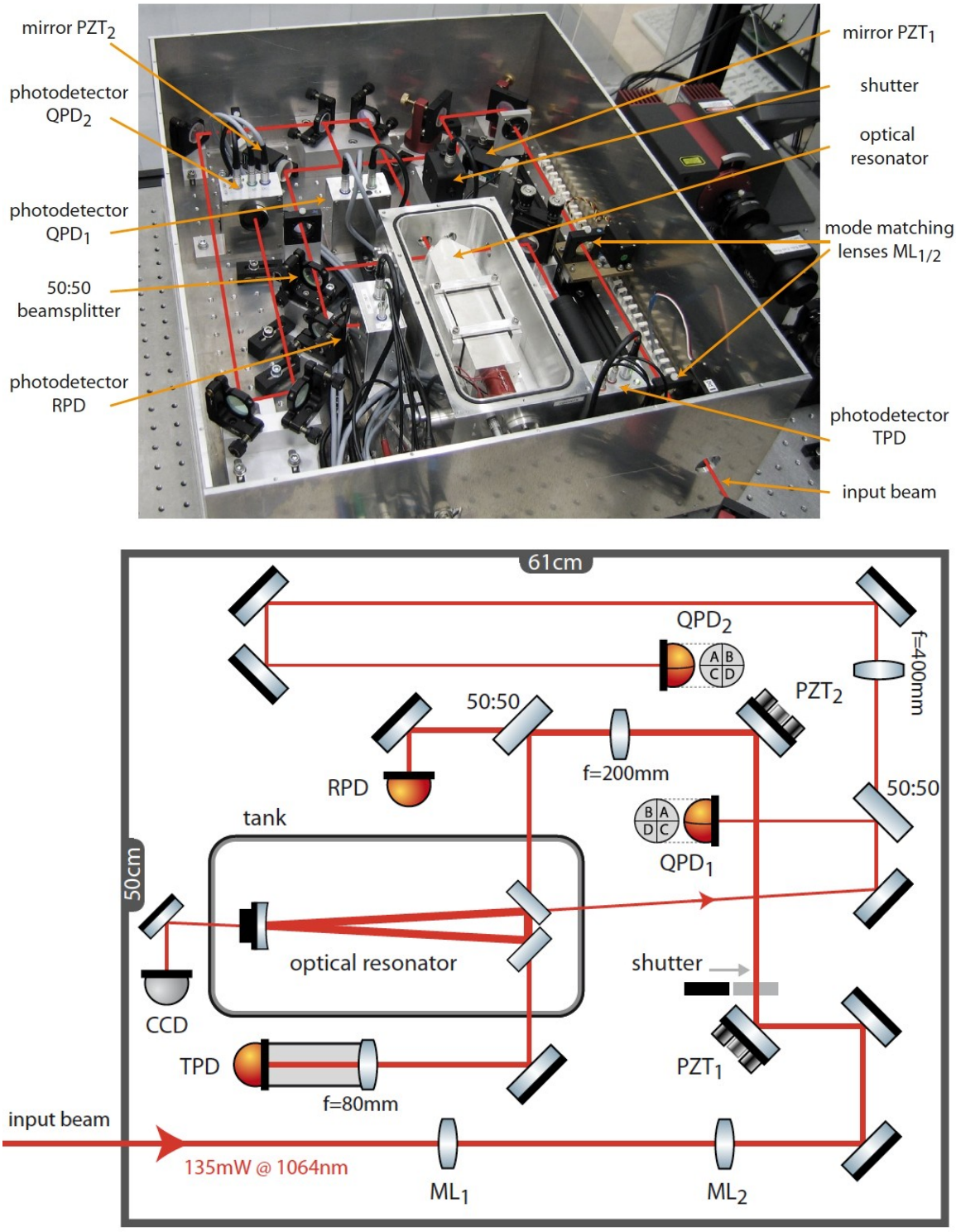

Figure 34. Photo and optical layout of the diagnostic breadboard.

6.2 PMC Diagnostics

Several parameters of the PMC are continuously measured to quickly identify problems concerning this optical resonator. Instrumentation is used to monitor the power downstream of the PMC, the PMC throughput, the spatial beam profile of the reflected and transmitted beam, and the PMC spacer temperature.

The power transmitted by the PMC and hand-off to the IO subsystem is monitored with one of the ISS inner-loop photodetectors (PD3 and PD4). The average power on the locking photodetector (PD2) of the PMC is used to measure the power reflected by the PMC. Both signals are available to CDS via the intensity stabilization servo (ISS) and PMC servo electronics. The throughput of the PMC can be calculated using both signals once they are calibrated. This signal is used for early identification of degradation of the PMC throughput caused by mode matching problems or resonator internal losses. Two CCD cameras (CCD3 and CCD5) are used to monitor the spatial beam profile of the transmitted and reflected beam of the PMC. The CCD camera for the transmitted beam is located after the low-power transmission port of the PMC. These video signals will be provided for display in the observatory, as is currently the case at LIGO Livingston. Furthermore the temperature of the PMC spacer is monitored to prevent too high a temperature and to provide diagnostics for the long range actuator of the PMC.

6.3 Reference Cavity Diagnostics

Some parameters of the reference cavity are monitored to identify problems. The photodetector (PD6) in transmission of the cavity, used for lock acquisition, is also used to monitor the power in the reference cavity. The average power of the photodetector (PD5) in reflection of the cavity, used for detecting the Pound-Drever-Hall signals, is used to diagnose the mode-matching and the power of the phase-modulation sidebands. A CCD camera (CCD4) in transmission of the cavity is used to monitor the resonant spatial mode of the cavity. This video signal will be provided for display in the observatory, as is currently the case at LIGO Livingston.

6.4 Control Loop Diagnostics

The performance and status of the control loops of the PSL (namely the inner loop and outer loop power stabilization, the frequency stabilization, the injection locking, and the PMC locking) are monitored with various signals that are available in the RTLinux system. The in-loop performance and potential saturations are monitored. Inputs for calibration signals in the analog control loops are provided to be able to continuously monitor the loop gain of each control loop. These signals are injected via the RTLinux system and the exact frequency and amplitude can be controlled by the RTLinux system. Furthermore, for the two power stabilization loops the performance is monitored with out-of-loop photodetectors, which independently measure the residual power fluctuations.

6.5 Room Camera Views

Camera views of the LAE and LDR and their associated ante-rooms will be required for equipment monitoring and personnel safety reasons. Such camera views are already installed at LIGO Livingston and have become useful for monitoring and status checking. These cameras will be located such that the zoom and panning features cover most of the area in question.

7 Computer Control and DAQ

7.1 Concept

The computer control of the PSL will be split in two layers. The first layer is the control of the laser itself including the injection locking control and the automated lock acquisition of the slave laser. This layer will use a commercial, real-time industrial control environment (Beckhoff TwinCAT) with AD, DA, and DIO modules called Beckhoff terminals. These terminals are located close to the devices under control and communicate with the Laser Computer via RJ45 and fiber links running a Beckhoff internal protocol (EtherCAT).

The second layer uses the standard aLIGO EPICS/RTLinux control environment which includes several computers (front end, EPICS client) and is summarized in the following as the *PSL Computers*.

A digital interface between the Laser Computer and the *PSL computers* will be available for the communication between the two layers. Besides the standalone mode, a remote control mode will be installed for the first layer. In this mode the Laser Computer will hand over some of its control authority to the *PSL computers*. In its initial configuration the *PSL computer* will only be able to shut down the Front End and high-power laser, close the Front End and high-power shutter, switch the injection locking loop and its ramp on or off and enable or disable the automatic lock acquisition of the injection locking loop. In case it is found during interferometer or PSL commissioning that more authority of the *PSL computer* over the laser is required this could be granted via a software change. Independent of the operational mode (standalone or remote) the *Laser Computer* will provide all important data characterizing the laser system to the *PSL computers* via this interface.

The *PSL computers* will control the FSS, ISS, PMC and the DBB. We will use analog control loops guided by the *PSL computers* for FSS, ISS and PMC control. The DBB will be fully controlled by the RTLinux system without any analog control loops.

During installation and maintenance phases, workstations or laptops will form the user interfaces to both layers in the LAE and LDR. These workstations will be shutdown during science mode operation.

7.2 Infrastructure

Figure 35 shows a layout diagram of the PSL control system. The PSL components are split in two locations: the laser diode room and the laser area enclosure (with the racks adjacent to the enclosure). The laser diodes are mounted on heat sinks in the diode boxes which themselves are mounted into a 19 inch rack. Each diode box has its own

Beckhoff terminal (BT) with AD and DA converters and DIO interfaces. The chillers are connected to a BT which is located in the so called interlock module in the LD rack 1. All BTs are connected via RJ45 cables to the LaserPC (labeled Beckhoff PC in Figure 35) which runs a program to control and monitor the temperature and power of each laser diode and which monitors the chillers. Furthermore a Beckhoff control box (CB) located in the second rack in front of the laser room is connected to the LaserPC via a fiber link. Workstations or laptops running the Beckhoff software can connect to the LaserPC to control and monitor all laser parameters. Standard user workstations can connect to the LaserPC via a terminal program (such as ULTRA VNC) from either the LAE, the LDR, the control room or more generally from anywhere within the CDS network in a read-only mode to get information on the laser status.

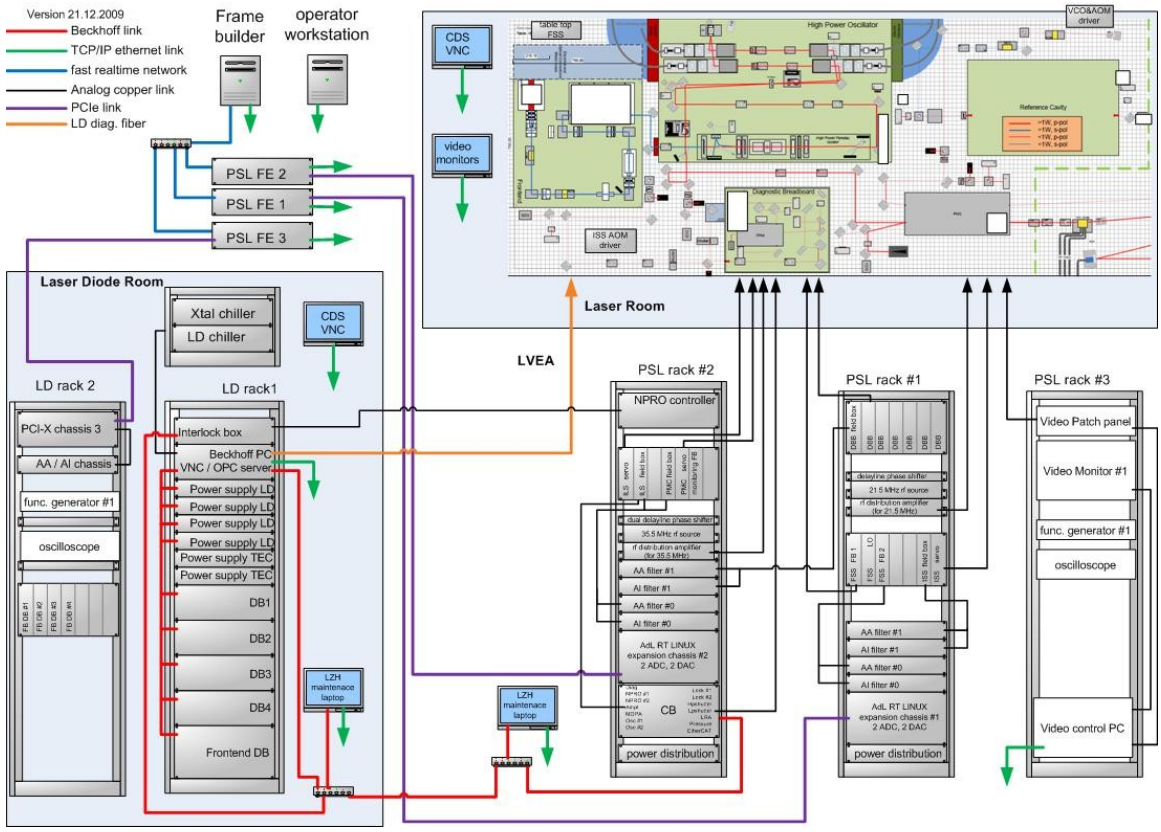

Figure 35. The layout of the PSL control system.

A standard aLIGO EPICS/RTLinux system (see AdvLIGO Control and Data System Conceptual Design LIGO T070059-v1) will provide interfaces in both locations. The RTLinux front end computers (FE) are connected via a PCI-X or PCIe connection to the PCI-X chassis which hold the AD/DA/DIO interface cards. The analog signals are connected via so-called field boxes to the anti-aliasing (AA) and anti-imaging (AI) filters

and from there to the interface cards. Signal conditioning like whitening and de-whitening will be performed in the field boxes.

Workstations to interface with EPICS or the real time front-end code will be available in both rooms. During Science Mode these workstations will be switched off and the laser will be controlled from the control room.

Three dedicated fiber links will be installed between the locations. One for the LaserPC running the TwinCAT protocol and one for the real time system to be used for the PCIe link of expansion chassis to the front end computer. The third will be used for applications running standard TCP/IP protocols. Each room needs a connection to the global CDS network.

7.3 TwinCAT Real-time Control

Both the eLIGO Laser and aLIGO Laser use an industrial real-time control software system by Beckhoff Automation known as TwinCAT (The Windows Control and Automation Technology). TwinCAT turns a PC into a real-time controller with a multi-programmable logic controller (PLC) system. Being an industrial system, it is highly robust and can continue operating even in the event of a Windows operating system crash.

7.3.1 EPICS and TwinCAT Interface

To facilitate monitoring of the laser performance, various signals acquired and controlled by TwinCAT are made available to EPICS via OPC. OPC (OLE[22] for Process Control) is a series of standard specifications between various industrial automation suppliers and Microsoft. It defines a standard set of objects; interfaces and methods for use in process control to provide interoperability and it is widely used in industrial environments. The OPC protocol is used to access TwinCAT process variables by application programs in a standard manner.

Software developed at the Berliner Elektronenspeicherring-Gesellschaft für Synchrotronstrahlung (BESSY)[23] allows direct access for EPICS records to process variables located on an OPC server. Figure 36 shows the communications links between the LaserPC and EPICS. The OPC server is located on the LaserPC. The iocShell is a core EPICS application and appears just like any Input/Output Controller (IOC) as in iLIGO. Familiar commands such as `dbl`, `dbpf` and `dbpr` work as for any other IOC. This has been installed and tested at the AEI and the LIGO observatories without any problems encountered thus far.

[22] Object Linking and Embedding (OLE).

[23] For further information see http://www-csr.bessy.de/control/SoftDist/OPCsupport/.

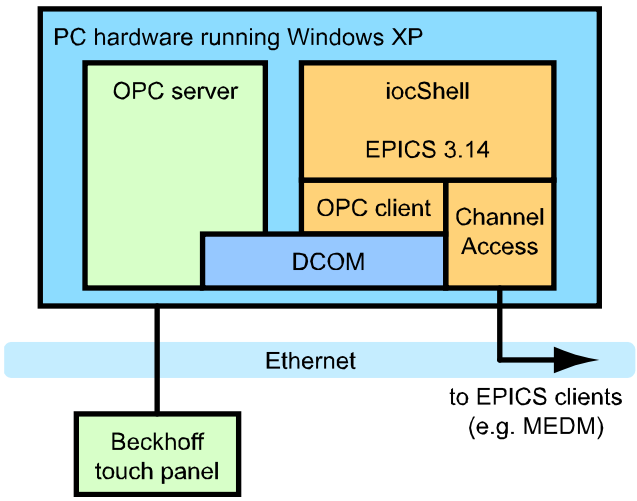

Figure 36. Communication between TwinCAT and EPICS via OPC. Running iocShell requires EPICS 3.14 and higher. EPICS records are then broadcast via channel access in the usual manner.

7.3.2 EPICS Records Mapping To TwinCAT Process Variables

EPICS records names are limited to 28 characters. No such length limit exists for TwinCAT process variables. To overcome this, a mapping file is used to map long TwinCAT process variable names onto EPICS records. Read and write access to the TwinCAT process variables is determined by access group and an access control list. Both the mapping and group file reside on the same PC as the OPC server. To ensure that data exported by the OPC server does not carry a time stamp different to the CDS DAQ system, EPICS record processing will determine the time stamp through the Time Stamp Event (TSE) field.

7.4 Control tasks and channel list

The following control tasks and DAQ monitoring channels are anticipated (for a detailed list of DAQ channels see the PSL interface document (aLIGO PSL interface document LIGO T0900644-v1).

7.4.1 NPRO (Beckhoff)

monitoring: laser diode (LD) temperatures, LD current, LD power, NPRO crystal temperature, NPRO power, interlock status

7.4.2 35W amplifier: (Beckhoff)

control: LD temperature control via digital control loop, setpoint control of LD current

monitoring: LD power sensed at the laser head (after optical fiber), 1064 nm power behind the first three amplifier heads, cooling water temperature, interlock status

7.4.3 35W amplifier: (RTLinux)

control: laser shutdown, closing the shutter

monitoring: relaxation oscillation monitor photodetector (includes the NPRO power monitor)

7.4.4 200W oscillator (Beckhoff)

control: LD temperature control via digital control loop, setpoint control of LD current, lock-acquisition automation of the injection locking (injection locking servo on/off, ramp generation, setpoint control of locking threshold), shutter control

monitoring: LD power sensed with LD internal diode, LD heat sink temperature, pump power per head (sensed after optical fiber), 1064nm output power (DC signal of injection locking diode), interlock status, injection locking status

7.4.5 200W oscillator (RTLinux)

control: laser shutdown, closing the shutter

monitoring: error point and control signal for injection locking, 1064 nm power, 1064 nm power reflected at Brewster plate

7.4.6 PMC(RTLinux)

control: lock-acquisition automation of the PMC locking (servo on/off, ramp generation, setpoint control for locking threshold), loop gain, switchable integrators, digital control loop for slow PMC temperature adjust

monitoring: transmitted power, error point and control signal of PMC controller, PMC spacer temperature

7.4.7 ISS (RTLinux)

control: servo on/off for outer and inner loop, servo gain control for outer and inner loop, DC reference setpoint control

monitoring: error points and feedback point of both loops, DC power behind PMC and modecleaner, AC fluctuations behind PMC and modecleaner

7.4.8 FSS (RTLinux)

control: , lock acquisition automation for FSS (servo on/off, ramp generation, setpoint control for locking threshold), servo gain control, offsets, modulation index, thresholds, tidal correction

monitoring: transmitted power, error point, feedback point, reference cavity temperature

7.4.9 DBB

The diagnostic breadboard will be fully automated by using the EPICS/RTLinux environment to perform a full characterization of the beam injected into the DBB. Remotely control shutters can be used to choose between either the beam leaving the 35 W laser or the 200 W beam. See DBB computer control manual (T0900579).

A channel list is defined in the PSL interface document (aLIGO PSL interface document LIGO T0900644-v1). This document will serve as a reference document for channel names, bandwidth and range, calibration and further information like channel descriptions etc.

Defining such a document as the reference will ease the electronic and wiring design and the programming of the control code and user interfaces.

8 Laser Area Enclosure

A schematic diagram of the Laser Area Enclosure (LAE) is shown in Figure 37. Particulate contamination on the optical surfaces exposed to the high-power laser beams has proved to be a critical issue for reliable operation of the AdL laser. A single dust particle can and has resulted in optics being damaged beyond repair. Therefore, the principal requirement of the LAE is to provide a dust-free working environment within which the PSL can be installed, commissioned, and maintained.

The concept for the LAE includes two rooms, the Laser Room and the Ante-room. The Laser Room is accessed via the Ante-room and the Ante-room is accessed via an air shower for personnel and small items or via double-doors for large items. There are two operating modes for the LAE, “Service Mode” and “Science Mode.” The facility is designed to Class 1000 standards when in the Service Mode with approximately 300 air changes per hour provided by HEPA filtered fan units (FFUs) mounted in the ceiling. In the Science Mode all FFUs in the LVEA are turned off and auxiliary HEPA filtered air is ducted to the Laser Room from a remotely located FFU. The Laser Room is designed to be very well sealed such that over-pressure can be maintained with a very low influx of outside air. The Laser Room provides 20 dB of acoustic attenuation for frequencies above 125 Hz when in the Science Mode.

In the Laser Room, return air is ducted through return air registers at the base of the walls, through the interstitial space, and into the intake air plenum which is located above the Laser Room. Motorized louvers or doors between the intake air plenum and the LVEA are closed during Science Mode operation to facilitate the 20 dB acoustic attenuation. In the Ante-room, the HEPA filtered air exhausts to the LVEA via dampers at the base of the Ante-room walls. These dampers close during Science Mode operation.

Stub walls extend from the bottom of the laser table to the LVEA floor on all four sides of the laser table support to provide a dust free interface between the Laser Room and the laser table support. The stub walls are set back from the edge of the table to provide toe kick space and space for electrical outlets and cable and water hose routing. Cables and water hoses are routed down off of the optical table then along the floor to the plan-east end of the optical table where they are routed across the floor to

the electronics racks or the LDR. This enables use of a rolling gantry-style lift to position heavy objects such as the 700 lb. high power oscillator box on the optical table. Electronics racks are located outside and adjacent to the LAE.

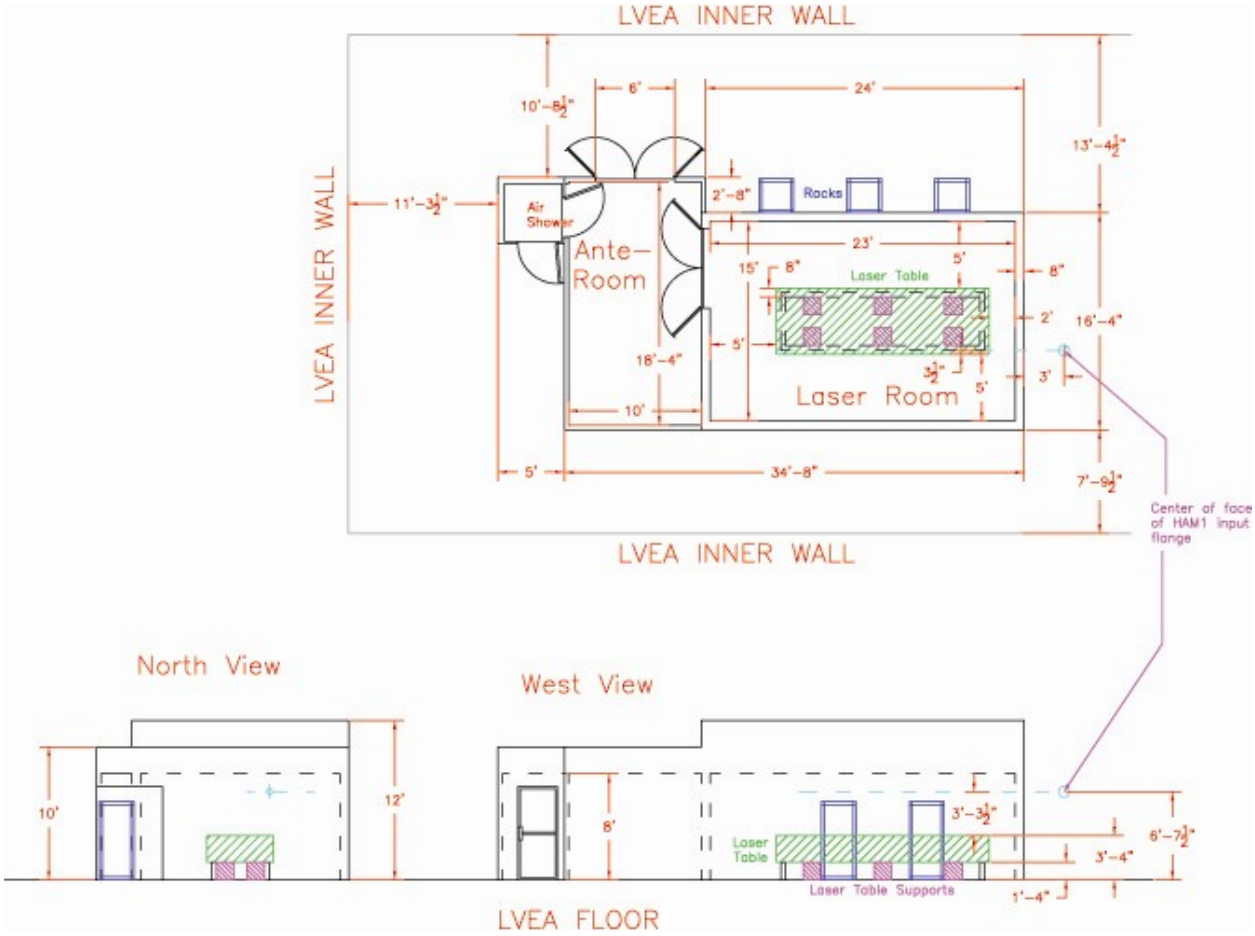

Figure 37. Plan and elevation views of the Laser Area Enclosure showing the Laser Room, Ante-room and air shower access. Both rooms are designed to Class 1000 standards with approximately 300 air changes per hour when operating in the Service Mode. A sealable intake air plenum above the Laser Room facilitates 20 dB of acoustic attenuation when operating in the Science Mode.